CHARACTERIZING THE PRO-SURVIVAL FUNCTION OF THE CUTA GROWTH ARREST SPECIFIC GENE IN QUIESCENT CHICKEN EMBRYO FIBROBLASTS

Disha Mehta, B. Sc.

A Thesis

Submitted to the School of Graduate Studies

in Partial Fulfilment of the Requirements

for the Degree

Master of Science

McMaster University

Descriptive Note

MASTER OF SCIENCE (2022) McMaster University

(Biology) Hamilton, Ontario

TTLE: CHARACTERIZING THE PRO-SURVIVAL FUNCTION OF THE CUTA GROWTH ARREST SPECIFIC GENE IN QUIESCENT CHICKEN EMBRYO FIBROBLASTS

AUTHOR: Disha Mehta, B.Sc. (McMaster University)

SUPERVISOR: Dr. P.A. Bédard

PAGES: ii, 85

Lay Abstract:

First characterized in *Escherichia coli* as a divalent cation tolerance protein, *cutA* has since been found to have a highly conserved trimeric structure and has been implicated in various different roles across species. Its characterization in eukaryotes, however, is not well defined. Gene profiling done by the Bedard Lab identified it as a gene that is found upregulated in density-arrested chicken embryo fibroblasts (CEF). In this study, we characterize its expression in reversible growth arrested CEF, as well as investigate its role in promoting cell survival in this state.

Abstract:

Genes expressed during quiescence, known as growth arrest specific (GAS) genes are of great interest due to their ability to prevent a cell from proliferating while enhancing its survivability by maintaining lipid homeostasis amongst other varied mechanisms. In response to nutritional stress, GAS genes may be upregulated, leading to quiescence instead of differentiation or senescence, implying that they are markers of quiescence. A GAS gene of particular interest is *cutA*. Gene profiling studies investigating gene signatures that are upregulated in response to quiescence inducing environments showed *cutA* to have a 50-fold increase in expression, one of the strongest responses to contact inhibition from the 28,000 genes that were analyzed. First characterized in *Escherichia coli*, as a divalent cation tolerance protein, *cutA* has a highly conserved trimeric structure across species, indicating a potentially fundamental role in cells. In this study, we confirmed the induction of *cutA* expression in response to oxygen depleted (hypoxia, contact inhibition) conditions that induce cellular quiescence, as well as in response to metal addition. We investigated the effect of aberrant *cutA* expression on cell proliferation and survival in quiescence by shRNA-mediated downregulation of the gene, which revealed that *cutA* does have a function in promoting cell survival in quiescence. Based on our findings, we propose a mechanism for the transcriptional activation of *cutA* in response to quiescent, and in response to metal addition.

Acknowledgements:

This project would have been impossible if not for the support, guidance, and encouragement from my supervisor, Dr. André Bédard. Dr. Bédard took me on as an undergraduate student with no research experience outside of the class. When I started working in his lab, I never expected the amount of hands-on training he would be providing personally. He collaborated on many experiments with me, teaching me to be a better researcher. His constant presence in the lab made him very accessible to his students that needed his help. Over the past three and half years, I have grown as a researcher, critical thinker, orator, and leader I knew I could always depend on him to answer my questions and listen to my struggles with experiments, unexpected results, and sometimes, even life. He always had amazing anecdotes to share from his time as a graduate student, which showed how devoted and passionate he was about science and research ever since then and they always inspired me to do better. Thank you for accepting me into your lab and always pushing me to go beyond what I thought was my best.

I also want to thank various others within the Department of Biology at McMaster. I would like to express my thanks to Haley, Kathy, and Rebecca for their assistance in all matters related to being a graduate student in a research-intensive program during a pandemic. Despite the plethora of questions, they always answered my questions. Thank you for helping me navigate the immense number of changes that came part and parcel with beginning my graduate journey in the middle of a pandemic. I had the pleasure of working for Alastair Tracey, Dr. Rosa DaSilva, Mihaela Georgescu, and various other sessional faculty, all of whom were always extremely encouraging and supportive. To the entire Bedard lab: Ronnie, Jordan, Preyansh, Zhouying, Emmerson, Ryyan, Hannah, Ali, Magda, Matthew, Henry, Daniel, and Natasha. Thank you for

sharing your knowledge and skills when I needed the help. I will cherish all the memories we made together as part of the lab. Your support and encouragement always bolstered me. Thank you to the entire biology graduate student community for being so amazing and welcoming. A special shoutout to my best friend, Kyle Amaral, who despite being on the other side of the country, was always ready to help me in any way that he could. Finally, I want to thank the most important person, my mother, Fenil. Thank you for your immense patience and kindness as I completed this project. Your love and support always got me through even the toughest times.

Table of Contents

List of Tables

List of Figures

List of Abbreviations

AChE	Acetylcholinestrase
BSA	Bovine Serum Albumin
CDK	Cyclin-Dependant Kinase
cDNA	Complementary Deoxyribonucleic Acid
C/EBP	CCAAT–Enhancer Binding Protein
CEF	Chicken Embryo Fibroblasts
C.I.	Contact Inhibited
CHM	Chicken Heart Mesenchymal cells
Cy	Cycling / Proliferating
DAPI	4',6-Diamidino-2-Phenylindole
DCFDA	2',7'- dichlorofluorescin diacetate
DMEM	Dulbecco's Modified Eagle Medium
DMSO	Dimethyl Sulfoxide
DNA	Deoxyribonucleic Acid
dUTP	Deoxyuridine Triphosphate
EDTA	Ethylenediaminetetraacetic acid
EST	Expressed Sequence Tag
ER	Endoplasmic Reticulum

ERK	Extracellular Signal Regulated Kinase
Ex-FABP	Extracellular Fatty Acid Binding Protein
FABP	Fatty Acid Binding Protein
FBS	Fetal Bovine Serum
G_1	Gap 1 Phase
G_2	Gap 2 Phase
G_0	Quiescence
GAS	Growth Arrest Specific
HBSP	HEPES Buffered Saline
HEPES	4-(2-hydroxyethyl)-1-piperazineethanesulfonic acid
HIF	Hypoxia Inducible Factor
HRP	Horse Radish Peroxidase
IgG	Immunoglobulin G
LTR	Long Terminal Repeats
M	Mitosis
MDA	Malondialdehyde
MRE	Metal Response Element
mRNA	Messenger Ribonucleic Acid
MTF	MRE-binding Transcription Factor

PBS	Phosphate Buffer Saline
PHD	Prolyl Hydroxylases
QRU	Quiescence Response Unit
RCASBP	Replication Competent ALV LTR with a Splice Acceptor Bryan Polymerase
RCF	Relative Centrifugal Force
RPM	Rotations Per Minute
RNA	Ribonucleic Acid
ROS	Reactive Oxygen Sequence
RSV	Rous Sarcoma Virus
S	Synthesis phase
SDS-PAGE	Sodium Dodecyl Sulphate Polyacrylamide Gel Electrophoresis
shRNA	Short Hairpin RNA
shRNAi	Short Hairpin RNA Interference
Src	Sarcoma
STE	Sodium Chloride-Tris-EDTA
TBS	Tris Buffered Saline
Tdt	Terminal Deoxynucleotidyl Transferase
TUNEL	Terminal Deoxynucleotidyl Transferase dUTP Nick End Labeling
TVA	Tumor Virus Receptor A

VHL	von Hippel Lindau

Vector Acronyms

RCASBP(A)	Control empty RCASBP(A) vector
RCASBP(A) – T2 *cutA* RNAi	RCASBP(A) vector containing one variant shRNA targeting *cutA*

Introduction:

1. Cell Cycle

i. Overview

The cell cycle, a ubiquitous and intricate process, is responsible for the growth and proliferation of cells. It is morphologically separated into interphase and mitosis, each of which can be further split into further distinct phases. Interphase consists of the three phases that prepare the cell for replication - gap 1 (G_1), synthesis (S), and gap 2 (G_2), and mitosis (M) consists of the four phases that segregate the mother cell into its two daughter cells – prophase, metaphase, anaphase, and telophase (Figure 1) (Schafer, 1998; Cooper, 2000; Lodish *et al.*, 2000; Barnum & O'Connell, 2014). The cell gains mass during the gap phases, while also providing time delay within which the cell can assess the internal and external environment to ensure that the conditions are ideal and all preparations have been completed before the cell commits to either the S phase or mitosis (Barnum & O'Connell, 2014). G_1 has rapid growth and elevated biosynthetic and metabolic processes to allow the cell to grow and prepare for DNA synthesis, and its duration depends on the external conditions relayed through extracellular signals (Schafer, 1998; Alberts *et al.*, 2002a; Barnum & O'Connell, 2014). The S phase is when most of the DNA synthesis takes place and is therefore the longest section of the cell cycle. During this phase, the cells have aneuploid DNA content, which is between 2N and 4N (Schafer, 1998; Cooper, 2000). G_2 increases the protein concentrations within the cell in preparation for mitosis (Alberts *et al.*, 2002a). A cell spends up to 95% of its time in interphase during each repetition of the cell cycle (Cooper, 2000). Following interphase, the four phases of mitosis will separate the replicated chromosomes with the help of a complex cytoskeletal mechanism – the mitotic spindle. These phases are followed by cytokinesis, which is the physical separation of the parent cell into two identical daughter cells, and this ends the cell cycle (Alberts *et al.*, 2002a).

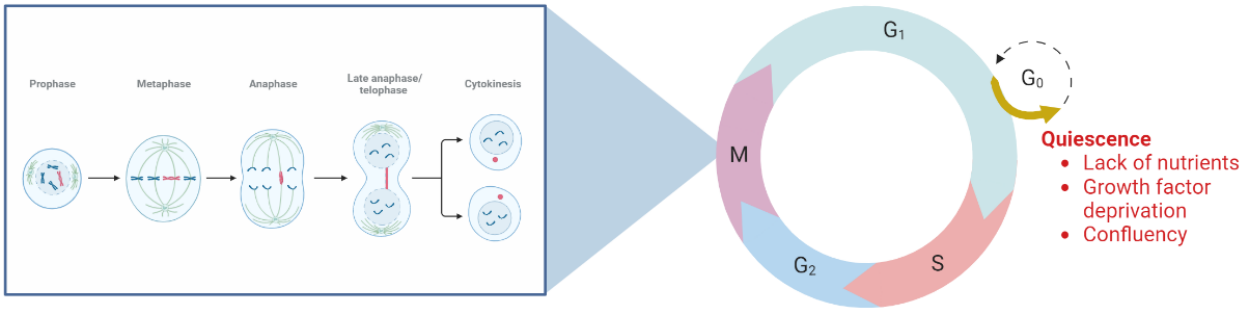

Figure 1. Cell cycle schematic. The cell cycle comprises of four distinct phases: Gap 1 phase (G_1), DNA synthesis (S), Gap 2 phase (G_2), and Mitosis (M). Mitosis has 4 phases - prophase, metaphase, anaphase, telophase/cytokinesis – which are responsible for the separation of replicated chromosomes and the subsequent separation of the parent cell cytoplasm, resulting in two identical daughter cells. In unfavorable conditions, a cell can exit the cell cycle and instead enter reversible growth arrest, a phase known as G_0, or quiescence. Quiescence is driven by a variety of factors such as nutrient limitations, contact inhibition, and growth factor deprivation, all of which prevent proliferation and promote survival.

ii. Cell Cycle Regulation

Progression through the cell cycle is driven by checkpoints, which are a series of control systems that enable proliferation only in the presence of stimulatory signals, ensuring the fidelity and integrity of the cell cycle (Barnum & O'Connell, 2014; Vermeulen, Berneman, & van Bockstaele, 2003) . The cell cycle is mainly catalyzed by complexes containing CDKs, which are serine/threonine protein kinases, and cyclins (Figure 2). The inactivation of CDKs prevents mitosis, making them crucial for progression through the cell cycle at specific points in the cell cycle, the checkpoints (Pines, 1995; van den Heuvel & Harlow, 1993). The checkpoints send signals which cause oscillations in CDK and cyclin concentrations and begin the process of advancing a cell into the next phase or preventing progression through the cell cycle. This process constitutes the phosphorylation of crucial substrates by CDKs (Kill & Hutchinson, 1995; Kato *et. al.*, 1993; McNally, 1996). These are present in abundance but are not

active unless bound by their related cyclin subunits, which are tightly regulated (Schafer, 1998; Alberts *et al.,* 2002b). Cyclin binding allows CDKs to conform to an active configuration similar to monomeric active kinases, which then promote DNA synthesis and progression through mitosis (Darzynkiewicz *et al.,* 1996; David-Pfeuty & Nouvian-Dooghe, 1996; Pines, 1991). In general, a cell can only enter the next cell cycle phase if the cyclin of the previous phase is degraded, and the next phase cyclin has been synthesized (Figure 2). Negative feedback ensures that the cell does not progress into the next phase until all stage specific conditions are fulfilled, with permanent changes ensuring that the cell does not return to a previous stage. CDKs are negatively regulated by the binding of inhibitory proteins, CKIs, that promote inhibitory tyrosine phosphorylation, blocking the phosphate transfer to the substrates. Negative regulators of the various cell cycle stages are distinct and work to inhibit the cell cycle differently. In G_2, phosphorylation of *cdk1* by *wee1* at tyrosine 15 (Y15) and threonine 14 (T14) residues in the active site, prevent the kinase activity of *cdk1*. In G_1 and S phase, inhibitors from the p16 and p21 families form stable complexes with CDKs and cyclins respectively, preventing the cyclins from binding CDKs and activating them (Barth, Hoffman & Kinzel, 1996; Guan *et al.,* 1994; Hirai *et al.,* 1995; Kamb *et al.,* 1994)**.** In this way, CDKs in concert with cyclins and their inhibitors work to halt the cell cycle if any phase does not progress to completion or if any cellular damage occurs, including but not limited to DNA damage or insufficient cell size (Schafer, 1998; van den Heuvel & Harlow, 1993; Barnum & O'Connell, 2014).

iii. Cell Cycle Checkpoints

Cell cycle checkpoints are "biochemical pathways that ensure dependence of one process upon another process that is biochemically unrelated" (Elledge, 1996, p). An example of this is a cell having to pass the DNA replication completion checkpoint before the biochemically unrelated process of mitosis

can begin. These checkpoints are not discrete points or times in the cycle but rather more nebulous and based on extracellular signals (Schafer, 1998). One of the most important cell cycle checkpoints is the cell size checkpoint, which occurs in late G_1 phase (Cooper, 2000). Controlling the size of the cell is critical to regulating nutrient distribution, as well as ensuring that each resulting daughter cell will be endowed with the appropriate amount of DNA as well as proteins and other biosynthetic material (Barnum & O'Connell, 2014). Growth factors will primarily act on the cells during G_1 and G_0 and after this the cells will no longer respond to the withdrawal of these factors, which point is known as the restriction point. Growth factors stimulate a cell to enter the cell cycle from G_0 and when withdrawn during early G_1, cause the cell to return to the G_0. However, when the growth factors are withdrawn during late G_1, when the cells have passed this restriction point, the cells will progress onto the S phase. Overall, the restriction point is therefore defined as "the point at G_1 at which commitment occurs and the cell no longer requires growth factors to complete the cell cycle" and is "temporally mapped at 2-3 hours prior to the onset of DNA synthesis" (Blagosklonny & Pardee, 2013; Barth & Kinzel, 1995; Schafer, 1998).

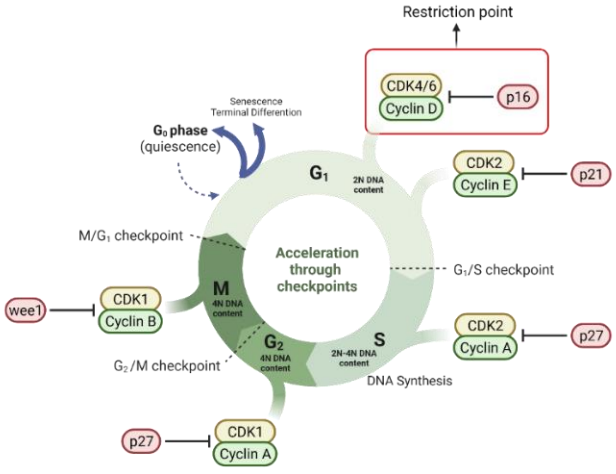

Figure 2. Cell cycle regulation schematic. Progression through the cell cycle is highly regulated by various CDK-cyclin complexes. Multiple checkpoints between each phase of the cell cycle ensure the fidelity and integrity of the process.

2. Cell Cycle Arrest (G_0)

i. Overview

Cell cycle arrest or delay in progression through the cell cycle results from a variety of factors that can be intrinsic or extrinsic and can affect any of the several different checkpoints (Schafer, 1998; Alberts *et al.*, 2002a; Cooper, 2000)). An intrinsic factor is cell size, which is important in determining cell cycle progression, particularly in yeast cells (Hayles & Nurse, 1986). An extrinsic factor is cell nutrition, which determines if and at what rate a cell will progress through the cell cycle (Hirst *et al.*, 1994; Shambaugh *et al.*, 1996). When a cell exits the cell cycle and enters a state of cell cycle arrest, it enters the G_0 phase. Cell arrest can be either reversible, which is known as quiescence, or irreversible, known as senescence. Senescence is the permanent exit of the cell from a cell cycle, which results in distinct phenotypic alterations (van Deursen, 2014). It is related to aging, wherein the replication rates diminish and then stop completely (Pack, Daigh, & Meyer, 2019). Senescent cells are characterized by increased cell size, as well as increased production of reactive oxygen species (ROS), lysosomes, and mitochondria, all of which contribute to the altered cellular phenotype (Cho & Hwang, 2012). Mechanisms including telomere shortening, and tumor associated stresses such as DNA lesions, mitochondrial dysfunction, and ROS induce senescence during the G_1, G_1/S, and G_2 checkpoints, causing the cells to lose their proliferative potential (Blagosklonny, 2011; van Deursen, 2014; Terzi, Izmirli, & Gogebakan, 2016). In contrast, quiescence is responsible for regulating proliferation by temporarily halting cellular growth in a specialized state known as G_0 (Cooper, 2000; Terzi, Izmirli, & Gogebakan, 2016). Quiescence occurs due to inadequate nutrition and or inadequate mitogens or growth factors (Figure 1) (Terzi, Izmirli, & Gogebakan, 2016). This state is characterized by the repression of growth factors as well as stimulation of those that inhibit growth, enhance cell survival, and prevent re-entry into G_1(Cho & Hwang, 2012; Erb *et al.*, 2016; Terzi, Izmirli, & Gogebakan, 2016). Further studies have found that different

quiescence signals result in growth arrest via different mechanisms, indicating that there are different quiescent states depending on the signals received (Coller, Sang, & Roberts 2006).

ii. Hypoxia and Contact Inhibition

A cell can enter a state of quiescence because of many different environmental signals. Two conditions found to promote quiescence are, low oxygen concentrations, hypoxia, and cell-cell contact, also known as contact inhibition (Erb et al., 2016.).

Oxygen is an important element to the survival of mammalian cells and as a result the cells have coping mechanisms that are induced in response to environmental deficit of oxygen (Chi *et al.*, 2006; Giaccia, Simon, & Johnson, 2004). The most important factors of this coping mechanism are the hypoxia inducible transcription factors (HIF), of which the primary factor is normally degraded during normoxia (21% O_2). During hypoxia, the different HIF factors form a functional and active complex, serving various functions including, promoting angiogenesis to scavenge oxygen, promoting transition to anaerobic metabolism and playing various roles in inflammatory responses (Carmeliet *et al.*, 1998; Chi *et al.*, 2006; Cramer *et al.*, 2003; gia *et al.*, 1997; Giaccia, Simon, & Johnson, 2004; Vaupel, 2004). Hypoxia has also been found to suppress senescence resulting from diverse stimuli, which inadvertently promotes quiescence. It does so by inhibiting mechanistic target of rapamycin (MTOR), which is responsible for cell growth in growth arrest and promoting senescence (Leontieva *et al.*, 2012). Apart from suppressing senescence, hypoxia also represses many genes that function to promote and/or regulate cell growth or proliferation, indicating that the cells are quiescent by inhibiting their progression through the cell cycle (Chi *et al.*, 2006).

The second environmental condition that promotes quiescence is cell-cell contact, also known as contact inhibition of proliferation, which is exhibited in fibroblasts that are in contact with each other

(Ribatti, 2017). Contact inhibition is characterized by the downregulation of genes like *cul-2*, *PCNA*, *lamin B*, and its receptor *CENPA*, all of which have been established as playing roles in controlling cell proliferation (Coller, Sang, & Roberts, 2006). Growth arrest resulting from contact inhibition cannot be reversed by refreshing nutritional serum, but instead the cells need to be sub-cultured at a lower population density (Gos *et al.*, 2005). Previous studies have shown that contact-inhibited cell experience hypoxia as well (Erb et al., 2016).

iii. Lipid Peroxidation

Lipids are integral elements within cells and have various fundamental functions. Polar lipids particularly are the structural components of cellular membranes and act as barriers for organelles (Ayala, Muñoz, & Argüelles, 2014; Mishra & Delivoria-Papadopoulos, 1989). During hypoxia, oxidative stress is exerted onto cells a as a result of the production and accumulation of ROS, which cause lipid peroxidation (Barrera, 2012b; Mansour & Mossa, 2009). The main sources of ROS include the plasma membrane, the endoplasmic reticulum, peroxisomes, and mitochondria. Lipid peroxidation occurs as a result of oxidation of lipids by ROS, particularly glycolipids, polyunsaturated fatty acids, cholesterol among others (Ayala, Muñoz, & Argüelles, 2014; Halliwell, 1991). Hydroperoxyl, a free radical, is the most potent oxidant causing lipid peroxidation, and can cause the attacked lipid, now a free lipid radical, to attack peripheral lipids, creating a chain reaction of lipid peroxidation, which can only be terminated by an antioxidant like Vitamin C (Ayala, Muñoz, & Argüelles, 2014). The cell responds to lipid membrane peroxidation based on metabolic circumstances and repair capabilities of the cell and can either promote cell survival or induce apoptotic measures. If the oxidative damage overwhelms the repair capacity of a cell, apoptosis is induced. Under low peroxidation rates, the cell induces maintenance and survival via constitutive antioxidants defense systems or signalling pathways to promote

upregulation of antioxidant proteins as an adaptive stress response (Ayala, Muñoz, & Argüelles, 2014; Halliwell, 1991).

3. Growth Arrest Specific (GAS) genes

i. Overview

All quiescent states in cells occur as a result of nutritional and/or mitogenic stress (Cho & Hwang, 2012). Genes that are overexpressed in response to nutritional stress include a group of genes known as growth-arrest specific (GAS) genes. These genes are downregulated during differentiation and senescence, indicating that their expression is linked to quiescence only (Fleming *et al.,* 1998). This differential gene expression allows the cells to survive in the unfavorable conditions induced due to mitogenic/nutritional stress by supressing growth and proliferation (Bedard *et al.*, 1987; Mao, Beauchemin, & Bedard, 1993). Their gene products can include proteins that negatively regulate cell proliferation, proteins with a high affinity for lipids, and survival factors, among others (Kim *et al.*, 1999). These genes also ensure that G_0 is reversible, doing so through various mechanisms, include the suppression of terminal differentiation (Coller, Sang, & Roberts, 2006). Bedard *et al.,* first identified and characterized a GAS gene product, p20k, expressed in chicken embryo fibroblasts (CEF) and chicken heart mesenchymal (CHM) cells (Mao, Beauchemin, & Bedard, 1993; Bedard *et al.*, 1987). Six GAS genes (*gas 1-6*) were found in a simple model system in 1988, some of which were rapidly downregulated upon induction of growth, while others took longer. They were found to be expressed in response to environmental stressors and antagonized proliferation as a result (Schneider, King, & Philipson, 1988). Further studies have determined that GAS genes play in role various other functions including, contributing to lipid metabolism, and protecting against oxidative stress resulting from free

radical buildup (Fornace *et al.,* 1989; Kim *et al.,* 1999; Melkonyan *et al.,* 1997; del Sal *et al.,* 1992; Schneider, King, & Philipson, 1988).

One of the best characterized GAS gene is *gas1*, an integral plasma membrane protein that is overexpressed during quiescence and inhibits the serum-induced transition from G_0 to S phase. It has been found to inhibit DNA synthesis, which prevents the cell from progressing through the cell cycle (del Sal *et al.,* 1992). The GAS genes also include SARPs, a family of secreted apoptosis related proteins, known to block the Wnt-frizzled signalling pathway, promoting cell survival by suppressing apoptotic signals (Melkonyan *et al.,* 1997). While essential to promoting cell survival in growth arrest, GAS genes, like the platelet-derive growth factor α-receptor (PDGFαR), are also necessary to reverse the growth arrest and facilitate the cell's re-entry into the cell cycle and making the cells competent (Lih *et al.,* 1996).

ii. p20K Lipocalin Expression and Regulation

A key GAS gene upregulated in during quiescence in chicken embryo fibroblasts (CEFs) is the p20K lipocalin, also known as extracellular fatty acid binding protein (EX-FABP) (Bedard *et al.,* 1987; Mao, Beauchemin, & Bedard, 1993). Lipocalins, which p20K is a part of, are a family of proteins with multiple conserved properties including the ability to bind hydrophobic molecules like long chain unsaturated fatty acids with high affinity, binding of cell surface receptors, and the formation of complexes with macromolecules (Cancedda *et al.,* 1996; Cancedda *et al.,* 1990.; Flower, 1996) .

p20K was first characterized as a secretory protein expressed by chicken heart mesenchymal (CHM) cells and quiescent CEF and has been found to be induced in quiescence and is upregulated in response to contact inhibition and hypoxia (Cancedda *et al.,* 1996; Erb *et al.,* 2016; Kim *et al.,* 1999). Subsequent studies have found p20K to promote cell survival, with the absence of its expression exhibiting increased lipid peroxidation and decreased cell survival (Erb, Msc. Thesis, 2016). p20K

expression is inhibited in actively dividing cells, as well as apoptotic and senescent cells, indicating that it is a marker of quiescence and is implicated in playing various roles depending on cell type, including cell survival in quiescent cells, as well as inflammatory response, and cell development in others (Cancedda *et al.,* 1996; Cancedda *et al.,* 1990.; Cermelli *et al.,* 2000; Descalzi Cancedda *et al.,* 2000; C. Gentili *et al.,* 2005; Gentili *et al.,* 1998; Kim *et al.,* 1999). It is also responsible for the metabolism of lipids and the transport of polyunsaturated fatty acids (Cermelli *et al.,* 2000; Descalzi Cancedda *et al.,* 2000). In conditions of hypoxia, quiescent p20K knockout cells exhibit an increase in apoptotic cell populations as well increased levels of lipid peroxidation, strongly establishing its role in promoting cell survival (Erb, Msc. Thesis, 2016.; di Marco *et al.,* 2003). Recent studies analyzing the crystal structure of p20K has revealed the presence of a multi-pocketed cavity that extends through the protein, encompassing ligand specificities for both bacterial siderophores and lysophosphatidic acid (LPA), indicating that p20K has dual functionalities, explaining its diverse roles, including its potential candidacy as an antibacterial catecholate siderophore binding lipocalin (Figure 3) (Correnti *et al.,* 2011).

p20K expression is dependent on the transcriptional activation of a 48bp region within the promoter, referred to as the Quiescence Responsive Unit (QRU) (Kim *et al.,* 1999; Mao, Beauchemin, & Bedard, 1993). CCAAT-Enhancer Binding Protein Beta (C/EBPβ) bound to this region causes upregulation of p20K, while the forced expression of a dominant negative mutant of C/EBPβ resulted in inhibiting p20K during quiescence (Figure 4A) (Kim *et al.,* 1999). Subsequent analysis of the QRU has revealed that it has two binding sites for C/EBPβ, which are labelled A and B respectively. QRU was found to be inhibited by linoleic acid, an essential fatty acid, and in cycling cells, by extracellular signal-related kinase 2 (ERK2), resulting in inhibition of p20K expression (Figure 4B). QRU is competitively bound by ERK2 and C/EBPβ during cell proliferation, with binding of ERK2 to the sequences that overlap C/EBPβ binding sites inhibiting p20K expression (Erb *et al.,* 2016).

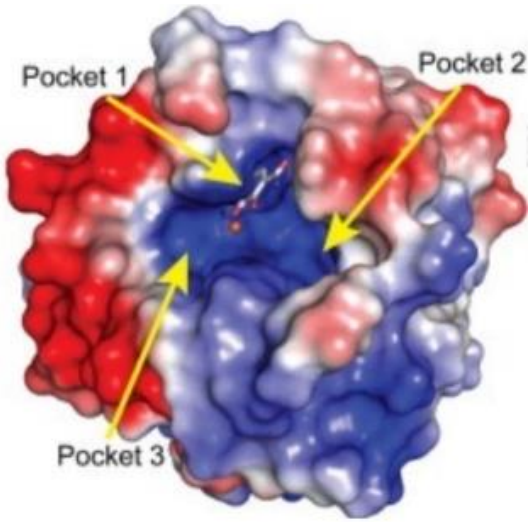

Figure 3: Crystal structure of p20K. The crystal structure, colored in electrostatic potential, of the p20K protein is shown, with arrows indicating the individual binding pockets in the p20K calyx (Adapted from Correnti et al., 2012).

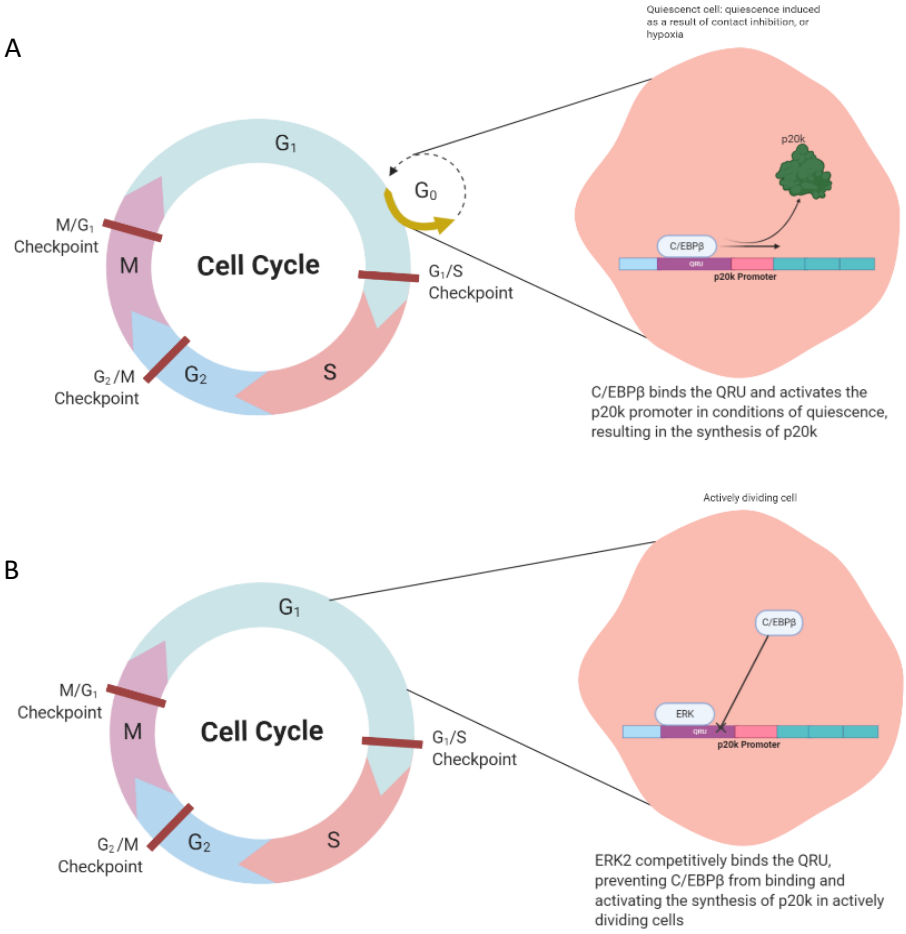

Figure 4. p20k synthesis is controlled by binding of transcriptional regulators to the QRU region in the promoter A) In density arrested induced quiescent CEF, C/EBPβ is synthesized and binds the QRU region on the p20k promoter as a trans-acting activator. This then initiates the synthesis of p20k in conditions of quiescence. B) In actively dividing cells, p20k synthesis is inhibited by the competitive binding of ERK2 to the QRU, which prevents C/EBPβ from activating the promoter by binding the QRU.

iii. CutA

CutA was first characterized in *Escherichia coli* as a divalent cation tolerance protein. Subsequent studies have found it to be strongly conserved across multiple species, ranging from bacterial to vertebrate species, implying that it has a fundamental function in cells (Fong, Camakaris, & Lee 1995; Zhao *et al.*, 2012). The *cutA* locus was found to contain three genes, one encoding a ~13 kDa protein (CutA1) located on one operon, and two that encode inner membrane proteins on the second operon (CutA2, CutA3). The localization of all three polypeptides varies with CutA2 and CutA3 localizing in the cell membrane while CutA1 is localized in the cytoplasm (Arnesano *et al.*, 2003; Fong, Camakaris, & Lee, 1995). When the locus was mutated, *E. coli* became increasingly sensitive to divalent metal ions – copper, zinc, nickel, cobalt, and cadmium (Fong, Camakaris, & Lee, 1995). When the Δ*cutA* was complemented with the ORF that encoded CutA1, it enhanced the tolerance, but only for Cd_{2+}. Only when complementation with both *cutA1* and *cutA2* genes was conducted, tolerance toward high Cu^{2+} and Ni^{2+} was restored (Fong, Camakaris, & Lee, 1995; Arnesano *et al.*, 2003; Selim et al., 2021). CutA is thought to be able to reduce excess copper ions in the cell by binding copper, since it has been observed to interact with copper in bacteria, or by affecting the import and export of copper by interacting with the cell membrane transporters (Fong, Camakaris, & Lee, 1995; Rensing & Grass, 2003). The first crystal structure of CutA protein was determined for *E. coli* (*Ec*CutA; PDB: 1NAQ) (Figure 5A) and for *Rattus norvegicus* (*Rn*CutA; PDB: 1OSC) (Figure 5B). Both proteins exhibit a trimer formation, indicating that this is an evolutionarily conserved protein architecture. In an *Ec*CutA crystal structure, a Hg^{2+} metal ion was found to be bound in one of the intersubunit clefts, and this was considered suggestive of CutA's involvement in heavy metal sensing and tolerance (Fong, Camakaris, & Lee, 1995; Selim *et al.*, 2021).

A cell's ability to tolerate the presence of cations is important to its functioning. Cations are required for cell survival and as such, cells need to be able to tolerate the cytotoxic nature of these cations that is

present regardless of concentration (Rensing & Grass, 2003). Metals like copper have been found to play roles in diseases like Parkinson's and cystic fibrosis, and as such require to be tightly regulated. However, these very metals are also required for crucial cellular processes like respiration and oxidative stress protection (Rensing & Grass, 2003). Oxidative stress and accumulation of ROS leads to lipid peroxidation, which can be potentially alleviated by CutA, a copper binding protein (Arnesano *et al.* 2003; Barrera 2012a; Rensing & Grass, 2003). Therefore, CutA can play a role in protecting against oxidative stress induced lipid dysregulation. Studies analyzing human genome have found overexpression of the CutA homolog, CUTA, exhibiting elevated levels of intracellular copper (Tanaka *et al.,* 2004). While CutA has primarily been found to be involved in copper transport and cation tolerance, it is also thought to help anchor acetylcholinesterase in neuronal cells, indicating another important potential function in cells (Navaratnam et al., 2000; Hou *et al.,* 2015). Based on the proposed role of CutA in anchoring AChE, as well as its involvement in copper tolerance in *E. coli*, and the general involvement of metal binding proteins in human neuronal pathologies, it has been speculated that a link exists between copper tolerance in bacteria and a potential role of CutA in mediating copper homeostasis in eukaryotic cells (Bush, 2000; Opazo et al., 2003; Arnesano et al., 2003).

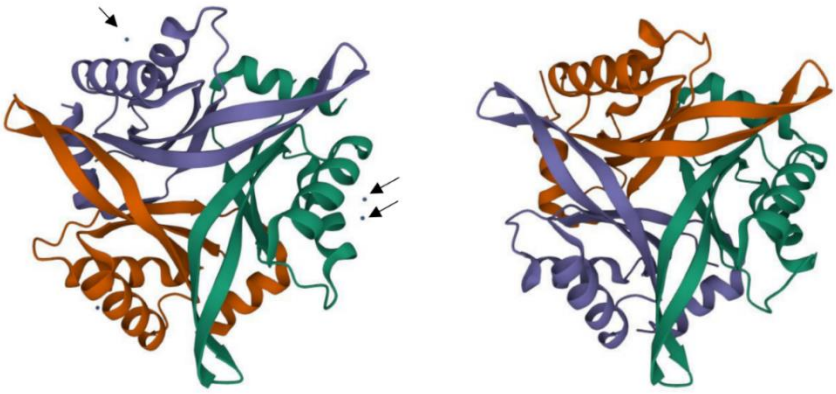

Figure 5. Crystal structure of CutA proteins. a) Crystal structure of CutA in *E. coli* (PDB: 1NAQ) with Hg^{2+} metal ions (indicated by black arrows) bound to the protein. b) Crystal structure of CutA in *R. norvegicus* (PDB: 1OSC)

Rationale and Objectives

Quiescence as a cell cycle phase is not well characterized. Past studies have only focused on serum starvation *in vitro*, a condition that is not physiologically ideal or accurate due to not being observed naturally. Contact inhibition, however. is observed in wound healing *in vivo*, and therefore serves as a more physiologically reliable model of growth arrest for *in vitro* investigations (Zegers et al., 2003). This condition is also associated with hypoxia, which indicates that hypoxic environments are also physiologically relevant to growth arrest (Erb et al., 2016).

In quiescence, a family of genes whose expression is upregulated is known as growth arrest specific (GAS) genes. GAS genes are a family of genes that are expressed in response to nutritional stress and ensure that quiescence is reversible. These genes, while downregulated during differentiation and senescence, are upregulated during quiescence, making their expression profile specific to quiescence **(citation)**. Previous studies conducted by the Bedard lab found p20K lipocalin gene to belong to this family and found it to be involved in promoting cell survival in quiescent CEF (Erb et al., 2016; Donders, MSc. Thesis, 2020). Subsequently, gene profiling was done by the Bedard lab to further identify genes that are differentially expressed when the cells become quiescent by either contact inhibition or serum starvation. There were distinct gene signatures belonging to particular pathways in the genes activated by contact inhibition. Gene signatures that were recognized included those activated in response to hypoxia or angiogenesis, those involved in signalling pathways, as well as genes involved in lipid metabolism and those regulated by C/EBPβ. Amongst the genes that were identified, *cutA*, initially annotated as an expressed sequence tag (EST), and later recognized as *cutA*, exhibited a 50-fold increase at the transcript level in density-arrested CEF, one of the strongest responses to contact inhibition from the 28,000 genes that were analyzed (Erb et al., 2016). This suggests that *cutA* is activated in response to quiescence

inducing environments that have oxygen depletion. Preliminary results confirmed that *cutA* expression is upregulated in hypoxic and contact inhibited CEF, whereas no expression is seen in cycling normoxic or serum starved CEF. This confirmed that *cutA* expression is akin to a GAS gene that is upregulated in response to exit from the cell cycle mediated by oxygen deprivation, but not in response to lack of nutrients, which sets it apart from the ER stress response.

In bacteria, *cutA* has been characterized as a divalent cation tolerance protein. Studies investigating its expression and function have found it to be expressed in the presence of metal treatments. Studies characterizing its structure have found heavy metal bound to the protein in the crystal structure in *E. coli*. Subsequent studies characterizing its structure in other bacteria, as well as eukaryotes have found that its trimeric structure is well conserved across species. In humans, its been suggested that *cutA* is involved in the anchoring of acetylcholinesterase in neuronal cells (Navaratnam et al., 2000; Arnesano et al., 2003; Hou *et al.*, 2015). Subsequent studies have implied the existence of a connection between its function in acetylcholinesterase anchoring in human neuronal cells and its suspected role in heavy metal tolerance due to the involvement of metal cations in neurological disorders (Arnesano et al., 2003). As a result of its structure being conserved across species, as well as its role in metal tolerance being seen across species, it can be suggested that in CEF, *cutA* might be induced in response to metal addition, and potentially also be involved in heavy metal tolerance.

Given the previous research on *cutA* as well as preliminary results obtained by the Bedard Lab, the primary goal of this study is to characterize expression and role of *cutA* in quiescent CEF. First, this study will characterize the expression of *cutA* in quiescent CEF, through analysis of western blots and immunofluorescence assays. It will aim to confirm preliminary results, showing expression induction in conditions of oxygen depletion as well as in response to metal treatment, as well as aiming to optimize treatments for further investigations. It will also examine intracellular localization of *cutA* in all

conditions that induce expression. The study will then assess the function of *cutA* in quiescent CEF through analysis of proliferation, apoptosis and reactive oxygen species (ROS) release in CEF with aberrant *cutA* expression. All together, the findings of this study will contribute towards forming a cohesive understanding of a GAS gene that is not regulated by C/EBPβ and its role in quiescent CEF as well as give insight into how it might be regulated.

Materials and Methods:

1. Chicken embryo fibroblast cell culture and culture conditions

Chicken embryo fibroblasts (CEF) were cultured in conditions of 41.5 °C with 5% CO_2 and 21% O_2 using Dulbeco's modified eagle medium (DMEM) high glucose 1x (Sigma D5546) supplemented with 5% heat inactivated cosmic calf serum (at 57 °C for 30 minutes, Hyclone AUA33984), 5% tryptose phosphate broth (Sigma T8782), 2 mM L-Glutamine (Gibco 25030), 500 units Penicillin and 500 µg Streptomycin (Gibco 15140). Near confluency, CEF were split into new cell culture plates using 0.05% Trypsin-EDTA (Corning 25-052-Cl) and STE prepared by the Bedard lab.

For normal, cycling (normoxic) conditions, CEF were cultured in conditions of 41.5 °C with 5% CO_2 and 21% O_2 and collected below 80% confluency. Samples were generated by splitting cells 16-20 hours prior to harvesting. For contact inhibited conditions, cells were cultured in the same conditions as normoxic CEF to 100% confluency. 24 hours prior to harvesting the CEF, the medium was changed to ensure saturation density, and incubated for 24 hours in the same conditions. For oxygen depleted conditions (hypoxia), CEF were incubated in 1.8% O_2 for 24-30 hours. The CEF were split 16-20 hours before incubation in hypoxic conditions, with cell confluency between 50-70%.

2. shRNAi Vector Transfection

2.1 Plasmid preparation

Replication competent ALV LTR with splice acceptor (RCAS) vectors were created by the Bédard Lab for CEF transfection based off constructs that were used by Kim et al. (Erb et al., 2016; Kim et al., 1999). The RCAS vector system was used to express shRNA to downregulate *cutA* expression in transfected CEF. The RCAS system is a molecular clone of the Rous sarcoma

virus (RSV) DNA genome, modified such that the *src* oncogene is replaced with a *Cla*I restriction site, allowing for the insertion of cDNA or shrRNA instead (Yang, 2002; Hughes, 2004). In this study, RCAS(A) vector was utilized, which expresses retroviral envelope A that is associated with the TVA receptor on the host cell surface (Figure 6) (Hughes, 2004).

Table 1: *cutA* oligonucleotide sequences

cutA-T1 shRNA forward	5'GAGAGGTGCTGCTGAGCGTAAGAGCTCGGCCTTGTATTTCTAG TGAAGCCACAGATGTA -3'
cutA-T1 shRNA reverse	5'ATTCACCACCACTAGGCACAAGAGCTCGGCCTTCTATTTCTAC ATCTGTGGCTTCACT -3'
cutA-T2 shRNA forward	5'GAGAGGTGCTGCTGAGCGCAACTATGTCAGATCCATCCATTA GTGAAGCCACAGATGTA -3'
cutA-T2 shRNA reverse	5'ATTCACCACCACTAGGCATAACTATGTCAGATCCATCCATTAC ATCTGTGGCTTCACT -3'
cutA-T3 shRNA forward	5'GAGAGGTGCTGCTGAGCGCAAGTGGAACTGTCCAACTATGTT AGTGAAGCCACAGATGTA -3'
cutA-T3 shRNA reverse	5'ATTCACCACCACTAGGCATAAGTGAACTGTCCAACTATGTTAC ATCTGTGGCTTCACT -3'
cutA-T4 shRNA forward	5'GAGAGGTGCTGCTGAGCGAAACTGTCCAACTATGTCAGATTA GTGAAGCCACAGATGTA -3'
cutA-T4 shRNA reverse	5'ATTCACCACCACTAGGCAGAACTGTCCAACTATGTCAGATTAC ATCTGTGGCTTCACT -3'

2.2 DNA Precipitation

A day prior to transfection, a total of 30 µg of DNA precipitate was prepared for each 100 mm cell culture dish that needed to be transfected. 10 µg of the plasmid construct DNA was brought up to a total of 30 µg with the addition of 20 µg salmon sperm carrier DNA and incubated in 0.2 M NaCl. Twice the total volume of 100% ethanol was added to the sample, and was left to precipitate overnight at -20 °C.

2.3 Calcium Phosphate Transfection

CEF were seeded on 100 mm tissue culture dishes on the day prior to transfection to ensure 50-70% confluency at the time of calcium phosphate transfection. Medium from theses plates was aspirate and replaced with 6mL of complete medium an hour prior to the transfection. The DNA precipitate solution made on the day prior was centrifuged at 14, 800 RPM (24, 532 RCF) for 15 minutes at 4 °C. The supernatant was removed, and the pellet was washed with 150µL of 70% ethanol and recentrifuged at 14, 800 RPM (24, 532 RCF) for 5 minutes. The ethanol was removed, and the pellet was vacuum dried for 2 minutes before being resuspended in 438 µL of ddH2O and 62 µL of 2M $CaCl_2$. The sample solution was added dropwise to 500 µL of 2X HBSP (1.5 mM Na_2HPO_4, 10 mM KCL, 280 mM NaCl, 12 mM Glucose, 50 mM HEPES, pH 7.12) while being vortexed. The mixture was inverted and then left to incubate for 20-30 minutes, after which, it was added dropwise to the cells in 100 mm culture dish and left to incubate for 4-6 hours before being glycerol shocked. For the glycerol shock, the medium was aspirated, and the were shocked for 90 seconds using 4 mL (per transfected plate) of a glycerol shock solution (15% sterile glycerol, 50% 2X HBSP, 35% ddH_2O). The glycerol shock solution was aspirated, and the cells were washed twice with complete medium after which they were incubated in 8mL of complete

medium in normoxic cell culture conditions. The cells were split and cultured for two passages before being used in further experiments.

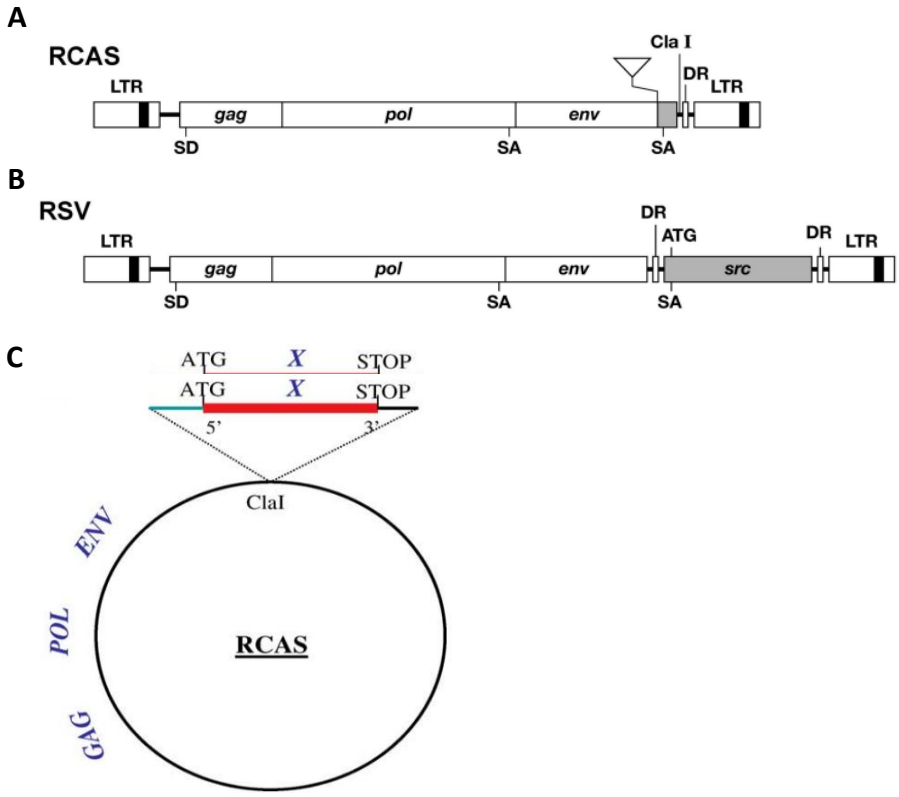

Figure 6. Schematics of replication-competent retrovirus RCAS. A) The proviral DNA, RCAS, inserted into the host chromosome. The long terminal repeats (LTRs), splice acceptors (SA), splice donor (SD), direct repeats (DR), and viral genes (*gag*, *pol*, *env*) are shown. The RCAS vector is a modified version of the RSV DNA genome, with most of the *src* gene deleted, replaced by a *ClaI* restriction site, and retaining only the src splice acceptor (Adapted from Hughes, 2004). B) Rous sarcoma virus (RSV) DNA with the *src* gene, which is modified to create the RCAS vector (Adapted from Hughes, 2004). C) A target sequence (denoted as X) can be inserted into the vector, which can then be transfected into replication competent cells, resulting in expression of the inserted sequence (Adapted from Yang, 2002).

3. SDS-PAGE and Western Blotting

3.1 Protein Sample Preparation

Following the cultivation of CEF under desired cultured conditions, they were washed three times with cold 1X phosphate-buffer saline [((PBS) - 172 mM NaCl, 2.7 mM KCL, 4.3 mM Na_2HPO_4, 1.47 mM KH_2PO_4, pH 7.4)]. Any remaining 1X PBS was aspirated from the samples followed by addition of 1 mL of fresh 1X PBS. The plates were then scraped with a rubber scraper to suspend CEF in the 1X PBS and transferred into a 1.5 mL centrifuge tube. The samples were centrifuged at 6500 RPM (4732 RCF) for 3 minutes in 4°C to collect the cells, after which the supernatant was removed. The cell pellets were resuspended in 1X Sodium Dodecyl Sulfate (SDS) sample buffer (10% glycerol, 5% β-mercaptoethanol, 2% SDS, 0.75% 0.0625 M Tris-HCl, pH 6.8) containing 1X Halt Protease and Phosphatase Inhibitor Cocktail (Thermo Fisher #78446), vortexed for 1 minute and then boiled for 2 minutes. Following cell lysis, the samples were centrifuged for 5 minutes at 14, 800 RPM (24, 532 RCF) to pellet insoluble debris. The supernatant was transferred to a new microcentrifuge tube and stored at -80°C for later use.

3.2 Bradford Assay

The protein concentration of the sample cell lysates was quantified using a Bradford Protein Assay. A standard curve comparing concentration (x-axis) to absorbance (y-axis) was created by combining increasing volumes (0-15 μL) of 1X bovine serum albumin (BSA-1 μg/μL) with 200 μL double distilled H_2O (or 200 μL − volume of BSA), 2 μL of sodium dodecyl sulfate (SDS), and 800 μL of Bradford reagent. Protein sample solutions were created with same composition of reagents and their respective concentrations as in the standard solutions, but with

the substitution of BSA and SDS for 2 µL of cell lysate. An Ultraspec 2100 Pro spectrophotometer set to the wavelength of 595 nm was used to measure the optical absorbance of the standards and the samples. The protein concentration of each sample was determined by comparing its absorbance to the standard curve using linear regression.

3.3 SDS-PAGE and Western Blotting

Total cell protein extracts (75 µg) were run on a 14% denaturing SDS-polyacrylamide gel along with a Precision Plus Protein Dual Color ladder (Bio Rad #1610374). The gel concentration was dependant on the protein size to be resolved. When resolved, the samples were blotted on to a nitrocellulose blotting membrane (Schleicher and Schuell, BA85) and subsequently blocked in a 5% solution of skim milk powder dissolved in 1X tris-buffered saline [(TBS) (20 mM Tris pH 7.6, 140 mM NaCl)] at room temperature for 30-60 minutes. The nitrocellulose membrane(s) were incubated with the desired primary antibody (see Table 2 for primary antibody concentrations) dissolved in 5% TBS milk overnight at 4 °C. The following day, the membrane(s) were subjected to a wash cycle consisting of two washes of 1X TBS, two washes of 1X TBST (1X TBS containing 0.1% Tween), and two washes of 1X TBS, each was done for 5 minutes. The nitrocellulose membrane(s) were then incubated in the corresponding secondary antibody solution (see Table 3 for secondary antibody concentrations) conjugated with horseradish peroxidase (HRP) combined with 5% TBS milk for 90-120 minutes at room temperature. The membranes were then subjected to the same wash cycle as described previously. The chemiluminescent signals were visualized via incubation with Luminata Forte Western HRP Subtrate (Millipore WBLUF0100) and imaged at various exposure times using hyperfilm (GE Healthcare #28906839) following the manufacturer's protocols.

Table 2: Primary antibody solutions for Western blotting

Antibody	**Dilution**
CutA (Lifetein, immunopurified)	1:75
ERK2 (SantaCruz, immunopurified)	1:1000
p20K (601-Y, Bédard Lab)	1:400

Table 3: Secondary antibody solutions for Western blotting

Antibody	**Corresponding Primary Antibody**	**Dilution**
Anti-Rabbit IgG, HRP-Linked Antibody (Cell Signalling #7074S)	CutA (Lifetein, immunopurified) p20K (601-Y, Bédard Lab)	1:25 000
Anti-Mouse IgG, HRP-Linked Antibody (Cell Signalling #7076)	ERK2 (SantaCruz, immunopurified)	1:25 000

3.4 Western blot and protein quantification

Quantification of Western blot protein samples for comparions was achieved using ImageJ software available on National Institutes of Health's (NIH) website. Exposed films were scanned and uploaded to ImageJ, and the band intensity for each Western blot was analysed as outlined in the ImageJ User Guide. Target protein expression was normalized using the expression of the loading control, ERK2.

4. Immunofluorescence (Intracellular localization) Assay

Intracellular localization of target gene was investigated using immunofluorescence techniques. CEF were seeded onto glass coverslips in 60 mm dishes and incubated in their

respective conditions (normoxia or hypoxia) for 24-30 hours. The coverslips were washed with sterile 1X PBS and the CEF were fixed utilizing 4% formaldehyde combined with 1X PBS for 30 minutes at room temperature. They were then washed with 1X PBS and subsequently permeabilized on ice using 3mL of permeabilization solution (0.1% Triton X-100 in 1X PBS) for 5 minutes. The coverslips were rinsed with 1X PBS and subsequently incubated in 5% fetal bovine serum (FBS) in 1xPBS for 1 hour at room temperature. The coverslips were rinsed with 1X PBS and then incubated in the desired primary antibody solution (see Table 4 for primary antibody concentrations) in 1X PBS overnight at room temperature. The following morning, the coverslips were rinsed with 1X PBS and then incubated in the corresponding secondary antibody (see Table 5 for secondary antibody concentrations) in 1X PBS for 2 hours at room temperature. The coverslips were then rinsed with 1X PBS and stained with Hoechst 33342 [(1.2 mg/mL diluted 1:300) (Thermo Fisher H1399)] for 2 minutes. The coverslips were rinsed with 1X PBS and then sterile ddH_2O, after which they were mounted onto glass slides using mounting solution and imaged using fluorescence microscopy.

To investigate intracellular localization upon metal addition, a known concentration of metal salt (here, $CuCl_2$) was added to CEF 24 hours after seeding on coverslips. Following this, the above-mentioned steps were utilized to investigate the intracellular localization.

Table 4. Primary Antibody Dilutions

Antibody	**Application**	**Dilution**
CutA (Lifetein, immunopurified)	Immunofluorescence	1:100
p20K (601, Bédard Lab)	Immunofluorescence	1:150

Table 5. Secondary Antibody Dilutions

Antibody	Application	Dilution
Daylight R488, IgG Lamin	Immunofluorescence	1:150

5. Proliferation assay

5.1 Standard Proliferation Assay

Cell proliferation and survival analysis was done by using confluent CEF from 100 mm plates to seed 24-well microtiter dishes and incubated for 24 hours to allow for cell adhesion. Following cell adhesion, the cells were incubated in their respective conditions, namely hypoxia (1.8% O2) and normoxia (41.5 ºC in 21% O2 and 5% CO2. Following incubation in the aforementioned conditions, cells were trypsinized with 500µL Trypsin-EDTA per well. The cell suspension was combined with 9.5 mL of ISOTON® II Diluent (Beckman Coulter 8546719) in plastic vials compatible for use with Z1 Coulter Particle Counter (Beckman Coulter, Coulter Corporation, Miami, FL), set to count particles within 12-20 µm. Cells were counted in quadruplicate after incubation of 0-, 24-, 48-, and 72-hour periods. Pairwise T-test statistical analyses were performed to compare samples.

5.2 Extended Proliferation Assay

An extended proliferation assay was done to analyze the effect of aberrant expression of *cutA* on cell proliferation and survival when returning cells to normoxic conditions post incubation in hypoxia. In order to analyze this, after incubation in hypoxia for 24- and 48-hours, cells were returned to normoxia for up to 48-hours. Cell counts were taken in quadruplicate every 24 hours upon return to normoxia, in addition to the cell counts for hypoxic and normoxic treated cells. The

assay was extended to 96 hours to accommodate cell counts for samples returned to normoxia post hypoxic incubation. Pairwise T-test statistical analyses were performed to compare samples.

6. TUNEL (Apoptosis Detection) Assay

Cellular apoptosis in transfected CEF was detected using TUNEL Assay (TUNEL assay kit – Abcam ab66108). Transfected CEF were seeded onto glass coverslips in 60 mm dishes and incubated in their respective conditions (normoxia or hypoxia) for 24-30 hours. The coverslips were washed with sterile 1X PBS and the CEF were fixed utilizing 4% formaldehyde combined with 1X PBS for 30 minutes at room temperature. They were then washed with 1X PBS and subsequently permeabilized on ice using 3mL of permeabilization solution (0.1% Triton X-100 in 0.1% sodium citrate) for 2 minutes. The coverslips were then rinsed with 1X PBS and the CEF were subsequently treated with terminal deoxynucleotidyl transferase (TdT) and TMR red fluorescent labeled dUTP for 1 hour at room temperature. The coverslips were rinsed with 1X PBS and the CEF were stained with Hoechst 33342 [(1.2 mg/mL diluted 1:300) (Thermo Fisher H1399)] for 2 minutes. The coverslips were rinsed with 1X PBS and then sterile ddH_2O, after which they were mounted onto glass slides using mounting solution. The samples were imaged in quadruplicates using fluorescence microscopy with 2000 cells counted per sample analyzed.

7. DCFDA Cellular ROS Detection Assay

The detection and quantification of ROS was evaluated using live cell DCFDA Cellular ros Detection Assay Kit (Abcam ab113851). CEF from confluent 100 mm dishes were used to seed 92 microwell plates, each sample seeded in sextuplicate. The plates were then incubated in normoxia for 24 hours to allow for cell adhesion, after which they are incubated in their

respective treatments (normoxia or hypoxia) for 24 hours. 1 hour prior to the end of the incubation period, cells were washed with 1X Buffer and stained with 25 µM DCFDA in 1X Buffer for 45 minutes in the respective incubation conditions of normoxia or hypoxia. The cells were the washed with 1X Buffer twice before a final volume of 100 µL of 1X Buffer was added to each well containing CEF. Fluorescent intensity was measured at Ex/Em = 485/535 nm using a plate reader. ROS levels were calculated after subtraction of background noise (blank well readings subtracted from all well measurements). ANOVA statistical tests were performed to compare the samples.

Results:

1. Characterization of *cutA* expression and intra-cellular localization in CEF

i. *cutA* expression is induced by contact inhibition, hypoxia, or in response to $CuCl_2$ treatment

Preliminary gene profiling studies had shown that *cutA* is upregulated in confluent CEF and in response to hypoxia, a condition resulting from high cell density (Erb et al., 2016). This suggests that *cutA* might be preferentially induced in response to hypoxia and contact inhibition, two conditions that result in cell quiescence. *cutA* is thought to be involved in heavy metal sensing and tolerance due to observed interaction between copper and CutA in bacteria, as well as the presence of Hg^{2+} metal ion in the crystal structure in *E. coli* (Fong, Camakaris, & Lee, 1995; Selim et al., 2021). Western blot analysis of cells grown in 21% O_2 normoxia, 1.8% O_2 hypoxia, with 10 µM $CuCl_2$ treatment, or to maximal confluence confirmed that *cutA* is not expressed in normoxic CEF but is expressed in response to contact inhibition, limiting concentrations of oxygen as well as when treated with 10 µM $CuCl_2$ (Figure 7A). CEF grown in hypoxia resulted in the strongest expression of *cutA*, with contact inhibited being the next highest, and $CuCl_2$ treatment having the lowest of the three conditions (Figure 7B). These results confirm that *cutA* is regulated as a growth arrest specific gene in CEF.

ii. Investigating induction time of *cutA* expression in CEF in response to hypoxia and in the presence of copper salts

Following the confirmation of *cutA* expression induction in quiescent CEF, time course experiment was conducted to investigate the induction time in response to hypoxia, as well as in response to the addition of copper. To do so, CEF were harvested at pre-determined timepoints

during either hypoxia or 10 µM $CuCl_2$ treatment. Western blot analysis done for hypoxia treated samples revealed that *cutA* expression is induced as early as 2 hours into hypoxia treatment, and reaches peak expression at 16 hours, remaining stable thereafter, with a slight drop in expression seen at 30 hours (Figure 8A-B). In response to 10 µM $CuCl_2$ treatment, Western blot analysis revealed that expression is seen induced as early as 4 hours into treatment, with expression peaking at 32 hours and beginning to slowly drop thereafter (Figure 8C-D).

iii. Investigating intracellular localization of CutA in CEF

cutA expression is induced in response to hypoxia as well as $CuCl_2$ but it's intracellular localization in CEF is unknown. To investigate this, immunofluorescence analyses were performed to localize CutA in CEF in normoxic conditions, hypoxic conditions and in response to addition of 10 µM $CuCl_2$ in hypoxia and normoxia. As a control, immunofluorescence analyses were also performed to detect p20K in the aforementioned cell conditions since its intracellular localization is known (Bedard et al., 1987). In normoxic CEF, no CutA or p20K was detected as expected. In hypoxia, p20K was detected in a localization consistent with the endomembrane system, particularly in the endoplasmic reticulum (ER) (Figure 9). CutA, however, is more widely distribute, showing both cytosolic and perinuclear staining (Figure 9). Precise identification of cellular compartments containing CutA would require positive co-localization with known markers for specific sub-cellular compartments (ER, Golgi, mitochondria, etc.)

In response to $CuCl_2$ treatment in normoxia, CutA was detected in the cell on the inside edge of the cell membrane as dense circular structures. It was also seen to be scattered around the periphery of the CEF (Figure 10A-C). In response to $CuCl_2$ treatment in hypoxia, CutA presence was detected as being scattered throughout the cytosol with greater concentration present near the

periphery, close to the cell membrane (Figure 10D-F). In response to $CuCl_2$ treatment, no p20K was observed in normoxia, or hypoxia (Figure 10G-L). Overall, immunofluorescence analyses showed CutA as having distinctly different intracellular localization in conditions that induce its expression, than what is known of p20K.

Experimental Figures:

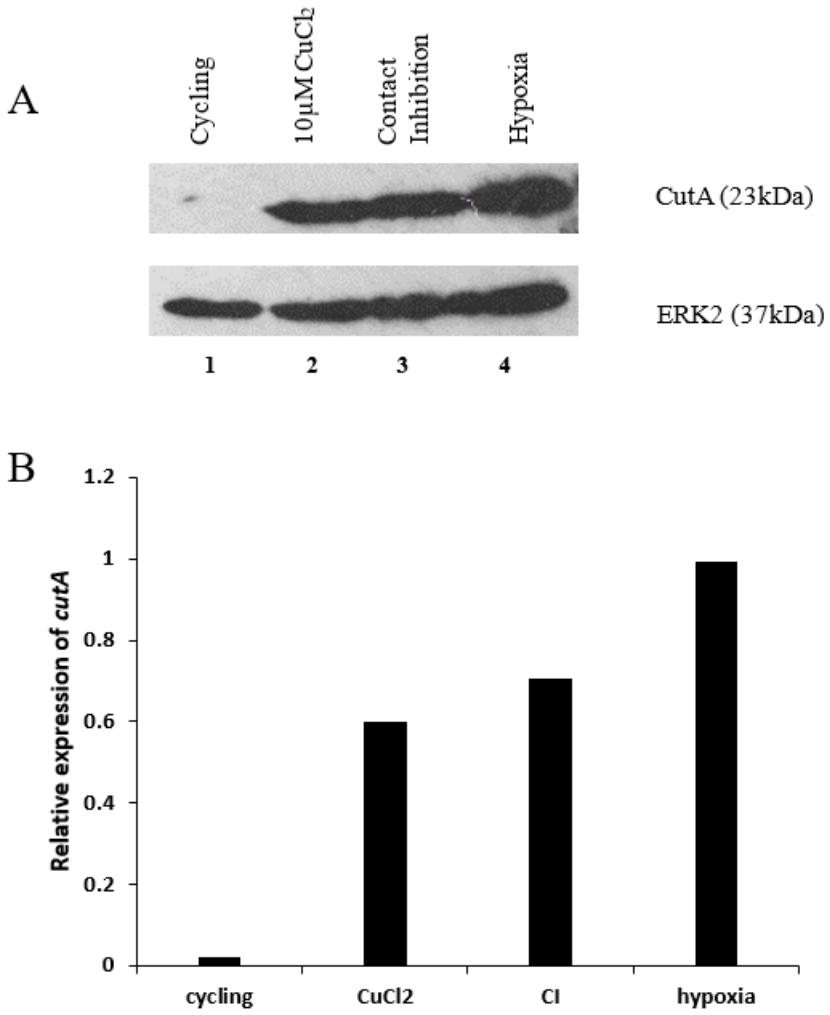

Figure 7: *cutA* expression is induced in response to hypoxia, contact inhibition, and CuCl2 (10 μM) treatment. A) Western blot analysis exhibiting the conditions that induce *cutA* expression. Loading control (ERK2) visualized to equalize expression level relative to protein loading. B) ImageJ analysis quantifying the relative level of expression of *cutA* in each condition that expresses it.

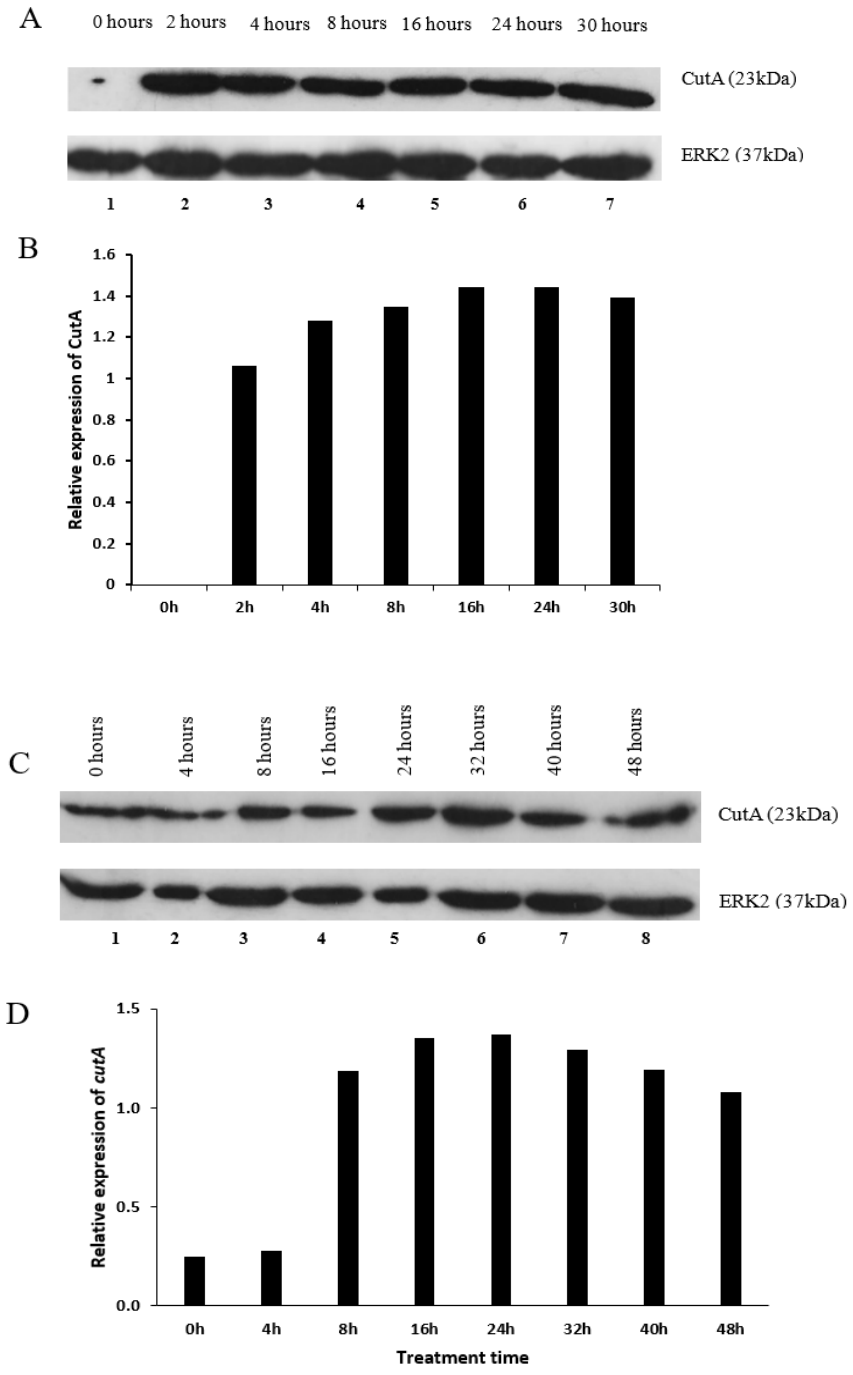

Figure 8: Investigating induction time of *cutA* expression in response to hypoxia or CuCl2 (10 µM) treatment in CEF. A) Western blot analysis looking at *cutA* expression induction time in response to hypoxia in CEF. Loading control (ERK2) visualized to equalize expression level

relative to protein loading. B) ImageJ analysis quantifying western blot of *cutA* expression induction time in response to hypoxia. C) Western blot analysis looking at *cutA* expression induction time in response to 10 µM CuCl2 treatment in CEF. Loading control (ERK2) visualized to equalize expression level relative to protein loading. D) ImageJ analysis quantifying western blot looking at *cutA* expression induction time in response to 10 µM CuCl2 treatment.

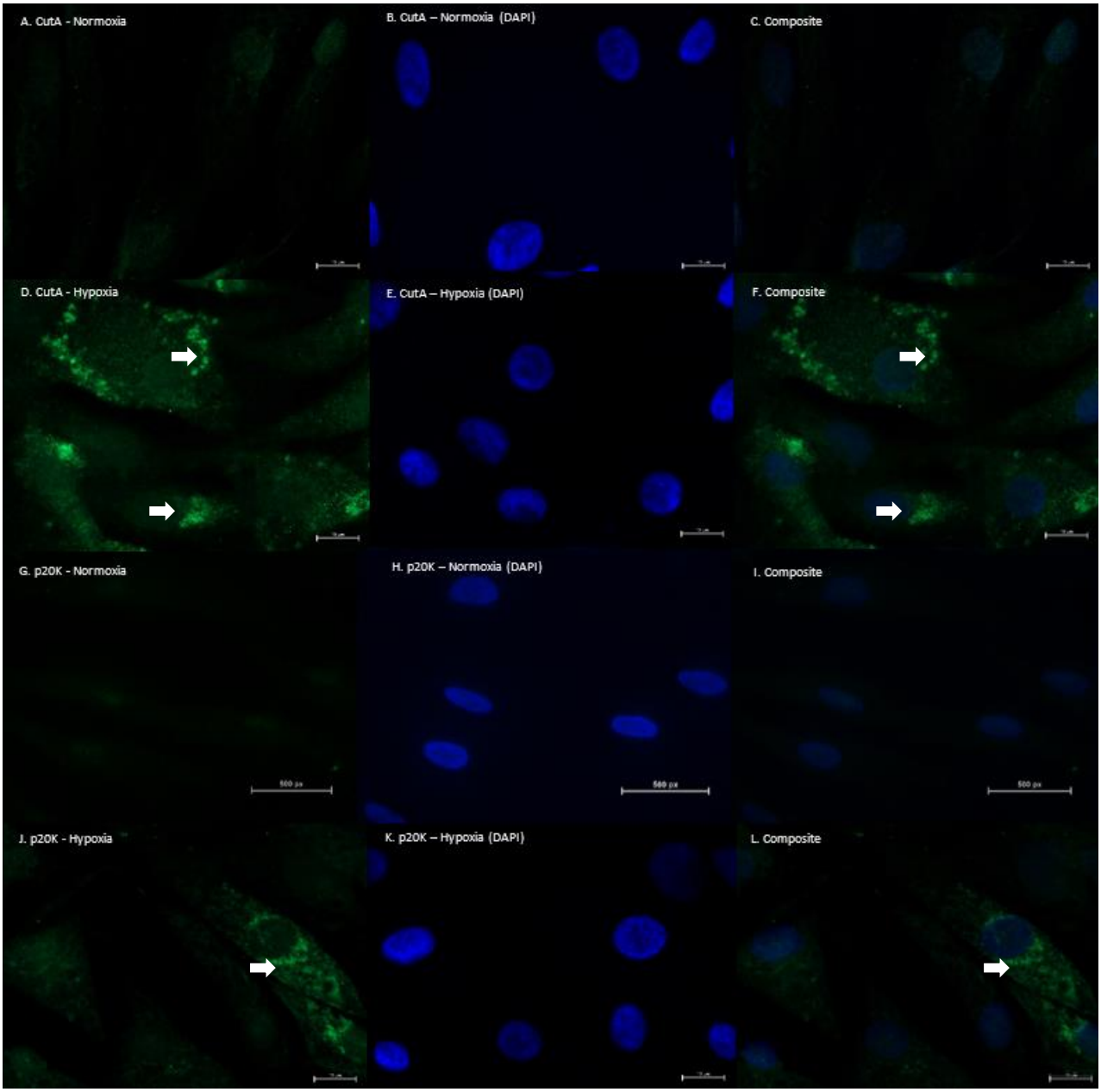

Figure 9: Immunofluorescence assay investigating the intracellular localization of CutA or p20k in normoxia or hypoxia, visualized at 100X. (A-C) Normoxic CEF stained for CutA. Panel A is showing CutA protein induction (indicated with white arrows), with panel B showing Hoechst staining of the cell nuclei. Panel C is a composite view of A and B. (D-F) Hypoxic CEF stained for CutA. Panel D is showing CutA protein induction (indicated with white arrows), with panel E showing the Hoechst staining of the cell nuclei. Panel F is a composite view of D and E. (G-I)

Normoxic CEF stained for p20K. Panel G is showing p20K induction (indicated with white arrows), with panel H showing Hoechst staining of the cell nuclei. Panel I is a composite view of G and H. (J-L) Hypoxic CEF stained for p20K. Panel J is showing p20K induction (indicated with white arrows), with panel K showing Hoechst staining of the cell nuclei. Panel L is a composite view of J and K.

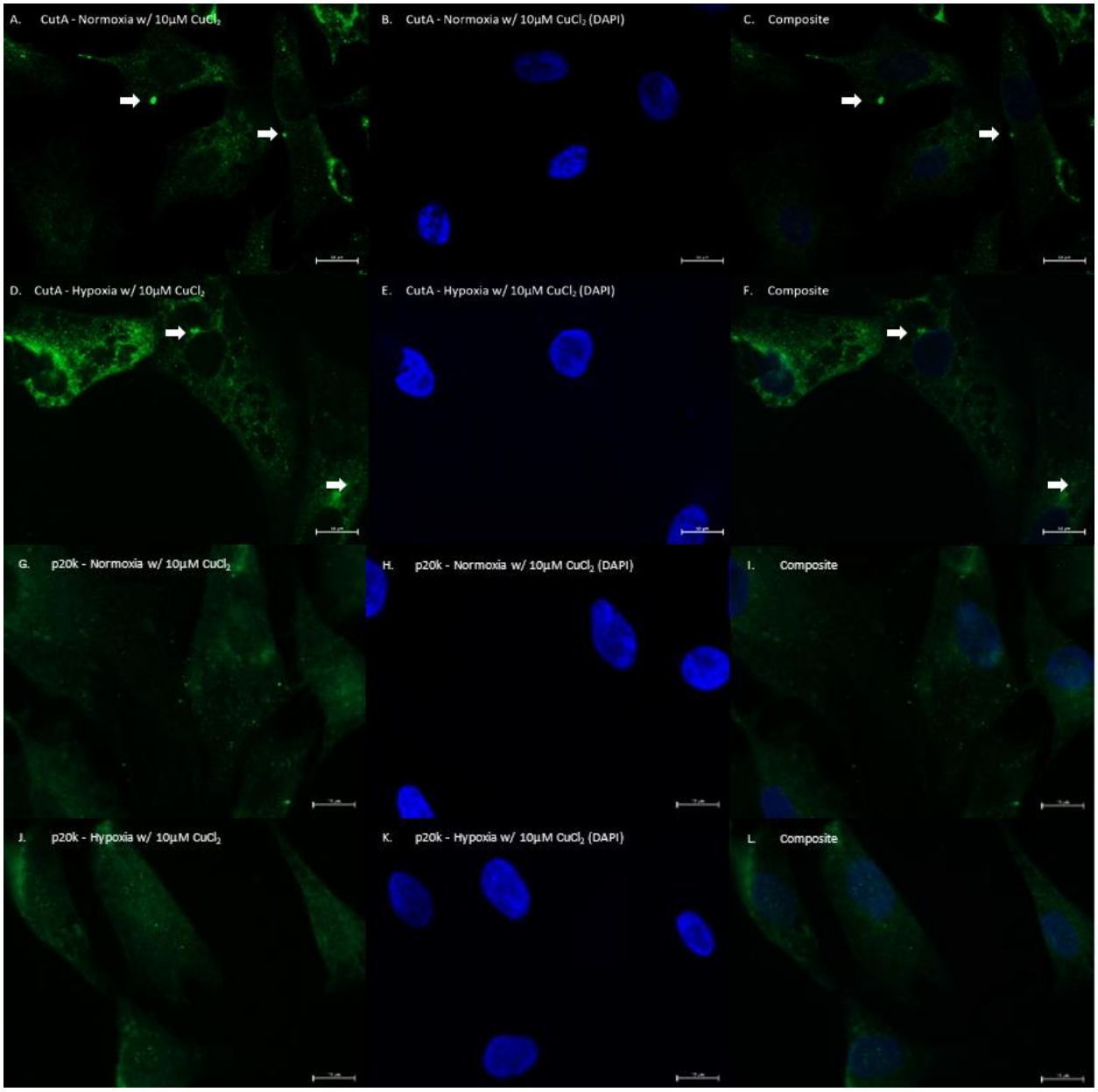

Figure 10: Immunofluorescence assay investigating the intracellular localization of CutA or p20k in normoxia or hypoxia, in presence of CuCl¬2 (10 µM), visualized at 100X. (A-C) Normoxic CEF treated with 10 µM of CuCl2 stained for CutA. Panel A is showing CutA protein induction (indicated with white arrows), with panel B showing Hoechst staining of the cell nuclei. Panel C is a composite view of A and B. (D-F) Hypoxic CEF treated with 10 µM of CuCl2 stained for CutA. Panel D is showing CutA protein induction (indicated with white arrows), with panel E

showing the Hoechst staining of the cell nuclei. Panel F is a composite view of D and E. (G-I) Normoxic CEF treated with 10 µM CuCl2 stained for p20K. Panel H is showing p20K induction (indicated with white arrows), with Panel H showing Hoechst staining of the cell nuclei. Panel I is a composite view of G and H. (J-L) Hypoxic CEF treated with 10 µM CuCl2 stained for p20K. Panel J is showing p20K induction (indicated with white arrows), with Panel K showing Hoechst staining of the cell nuclei. Panel L is a composite view of J and K.

2. Functional characterization of *cutA* in CEF

i. Downregulating *cutA* expression to investigate its role in quiescent CEF

Genetic tools can be used to alter the expression of *cutA* to study its function in growth arrested cells. Consequently, retroviral RCASBP vectors were created to downregulate *cutA* expression in CEF. Replication-competent viruses encoding shRNA specific to *cutA* were used to obtain *cutA* downregulation and examine the function of this protein in hypoxia, contact inhibition, and in response to the addition of copper. Various vectors were created, such that they targeted different regions of the *cutA* transcript, and tested, resulting in one vector being identified (*cutA* T2) as successfully being able to consistently downregulate expression. CEF were transfected with group A retroviral vector as a control (RCASBP(A)) or the shRNA construct for *cutA* downregulation (RCASBP(A)-*cutA* T2 RNAi) and incubated in normoxia, hypoxia, or to maximal cell confluence. Western blot analysis of samples obtained from the aforementioned CEF confirmed that *cutA* is not expressed in normoxic CEF, and that there was no expression observed in shRNA expressing CEF populations, even in conditions of oxygen deprivation (24 hour 1.8% O_2 hypoxia and maximal confluence) (Figure 11A-B). In contrast, control populations showed strong induction of *cutA* in response to 24 hours of hypoxia, or proliferation to maximal confluence, i.e., contact inhibition (Figure 11A-B).

ii. shRNA mediated downregulation of *cutA* does not influence the expression of p20K lipocalin, a GAS gene, in quiescence induced in response to the oxygen deficient conditions of hypoxia and contact inhibition

p20K lipocalin also known as EX-FABP, is a key GAS gene found to be upregulated during quiescence. It was first characterized as a secretory protein and cell-associated in chicken heart mesenchymal (CHM) cells and since then has been found to be upregulated in hypoxia and contact inhibition in CEF. It is known to be regulated by C/EBPβ, which acts as its transcriptional activator and binds to the QRU to induce expression. It is also known to share a regulatory pathway with FABP4, another lipocalin that is regulated by C/EBPβ, wherein downregulating expression of either, results in reduced expression of the other. In CEF, upon shRNA-mediated inhibition of lipocalins, CEBP/β activity is inhibited, which in turn results in downregulation of its target genes (p20K, FABP4). Investigations into how this affects the other GAS genes was done by looking at the effect of downregulating lipocalins on *cutA* expression due to it not being involved in lipid homeostasis and its structural difference from the lipocalins. Results show that shRNA mediated downregulation of either lipocalin had no effect on the expression of *cutA*, which suggested that the overall GAS response was not impacted (Moftakhari et al., in preparation). The question, however, remains as to whether shRNA mediated downregulation of *cutA*, has any impact on the expression of these CEBP/β regulated lipocalins. To address this, western blot analysis was done, which showed no loss of p20K expression in conditions of hypoxia and contact inhibition in either the control or shRNA expressing cells (Figure 11A,C).

iii. Investigating the effect of *cutA* expression on proliferation and survival of CEF in quiescence

After successful characterization of the shRNA construct and its ability to downregulate *cutA* expression irrespective of cellular and environmental condition, the proliferative capacity of cells was measured to characterize the impact of *cutA* on cell proliferation and survival in hypoxic environments. To do so, the accumulation of cells infected with the control RCASBP(A) vector was measured and compared to that of cells infected with the shRNA construct, in conditions of normoxia and hypoxia. RCASBP(A) controls exhibited normal proliferation in normoxic conditions over a 72-hour time period, while cells with *cutA* shRNA exhibited similar proliferative rate analogous to the control up to the 48-hour mark but was significantly lower at the 72-hour timepoint (Figure 12). This timepoint corresponds to saturation density i.e., levels of CEF observed at contact inhibition (data not shown). All cells displayed a reduced proliferative capacity in hypoxia when compared to their counterparts incubated in normoxia. However, CEF with the *cutA* shRNA displayed a marked reduction in cell numbers at the 48 and 72-hour timepoints compared to the control populations, which displayed an increased cell number, albeit at a markedly reduced level. (Figure 12). Of note here is that all cell groups began with analogous population sizes, signifying that the difference seen here is not a result of initial variations in cell population density. The trend observed with the *cutA* shRNA populations is reminiscent of what has been seen in p20K shRNA cells and FABP4 shRNA cells, all of which display lower cell numbers in hypoxia in contrast to the control (Moftakhari et al., 2022, in preparation).

To complement the proliferation assays, a different version of it was conducted, wherein hypoxic CEF were returned to normoxia after 24 and 48 hours of exposure for a total of 96 hours after seeding. This was done to investigate whether the re-entry into the cell cycle was impaired

after downregulation of *cutA* i.e., whether they are able return to proliferating upon normal conditions being re-established. It was seen that with control CEF, upon being returned to normoxia after either 24 or 48 hours, they begin to proliferate normally. In contrast, CEF with *cutA* shRNA show a marked decrease in cell population while in hypoxia, which continues even upon being returned to the normoxic environment (Figure 13).

cutA has also been speculated to be involved in heavy metal sensing and tolerance. Previously, it has been shown that *cutA* is induced in CEF in response to $CuCl_2$ treatment (Figure 7) and that its intracellular localization is also impacted in those conditions (Figure 10). To further investigate the function that *cutA* plays in relation to metal salts, a proliferation assay was done to determine whether *cutA* expression promotes cell survival in the presence of $CuCl_2$. Two different concentrations of $CuCl_2$ were used, 10 µM and 50µM. Preliminary results from this show that 50µM treatment had a greater effect on cell accumulation and survival than 10 µM treatment. In shRNA expressing cells, both treatment concentrations resulted in reduced cell numbers compared to control cells, which were proliferating normally (data not shown). However, cells treated with 50µM $CuCl_2$ had an overall significantly lower cell count, irrespective of timepoint and cell group, when compared to those treated with 10 µM $CuCl_2$ (Figure 22, data not shown). The difference between cell count was more distinct for cells treated with 10 µM $CuCl_2$, perhaps due to this concentration being one that induces the highest level of *cutA* expression (Figure 23, data not shown). This preliminary data suggests that *cutA* does promote cell survival in the presence of $CuCl_2$.

iv. Investigating effect of *cutA* expression on cell survival in quiescence

As *cutA* might have a pro-survival function in conditions of quiescence, this may explain the reduced cell population seen in hypoxic cells with *cutA* downregulation. To investigate cellular viability in cells with aberrant *cutA* expression, TUNEL assays were conducted with sub-confluent control and *cutA* shRNA CEF in normoxia and hypoxia. Apoptosis was quantitated by two different criteria i.e., TUNEL positivity, and chromatin condensation/nuclear fragmentation, as determined by Hoechst staining. The prevalence of cell apoptosis was low in hypoxic control cells, indicating that our conditions of hypoxia are well tolerated in CEF. Insignificant levels of apoptosis were noted in populations incubated in normoxic conditions (Figure 14). In contrast, the incidence of apoptosis was markedly higher in *cutA* shRNA CEF incubated in hypoxia (Figure 14). An approximate 8-fold increase in apoptosis was observed upon *cutA* downregulation, with less than 1% of control cells undergoing apoptosis in hypoxia (Figure 14). TUNEL-positive cells displayed nuclear fragmentation or chromatin condensation, which was visualized with Hoechst 33342 fluorescent stain. This is analogous to what was seen with p20K shRNA cells and FABP4 shRNA cells grown in hypoxia, both of which displayed increased incidence of apoptosis, 6.5-fold and 7-fold, respectively, when compared to the control (Moftakhari et al., 2022, unpublished). This signifies that *cutA* has a pro-survival function in hypoxic conditions.

v. Effect of *cutA* expression on reactive oxygen species (ROS) prevalence in quiescent CEF

Previous studies have found increased ROS production resulting from shRNA mediated downregulation of GAS genes (Moftakhari et al., 2022, in preparation). Increased ROS are associated with oxidation of lipids as well as other key macromolecules, resulting in aberrant cell growth and development (Juan et al., 2021). To investigate whether *cutA* plays a role in alleviating

oxidative stress resulting from increased ROS production, ROS prevalence was analyzed in hypoxic CEF displaying *cutA* downregulation. To do so, a DCFDA/H2DCFDA fluorogenic dye was used, which serves as an indicator of hydroxyl, peroxyl, and other ROS production in cells. A significant surge in ROS level was noted in hypoxic samples lacking *cutA* in contrast to their normoxic counterparts, approximated to be 1.8-fold (Figure 15). In comparison, no marked difference was noted in ROS production in control cells between the two conditions (Figure 15). A substantial increase in ROS prevalence was noted in hypoxic *cutA* shRNA when compared to hypoxic control cells, which was approximated to being a 3.3-fold difference (Figure 15). This is reminiscent to what was seen with p20K shRNA cells and FABP4 cells, which showed marked increase in ROS accumulation when compared to control samples (Moftakhari et al., 2022, in preparation). This suggests that *cutA* alleviates oxidative stress by mitigating ROS production and promoting cell survival in hypoxic conditions.

Experimental Figures:

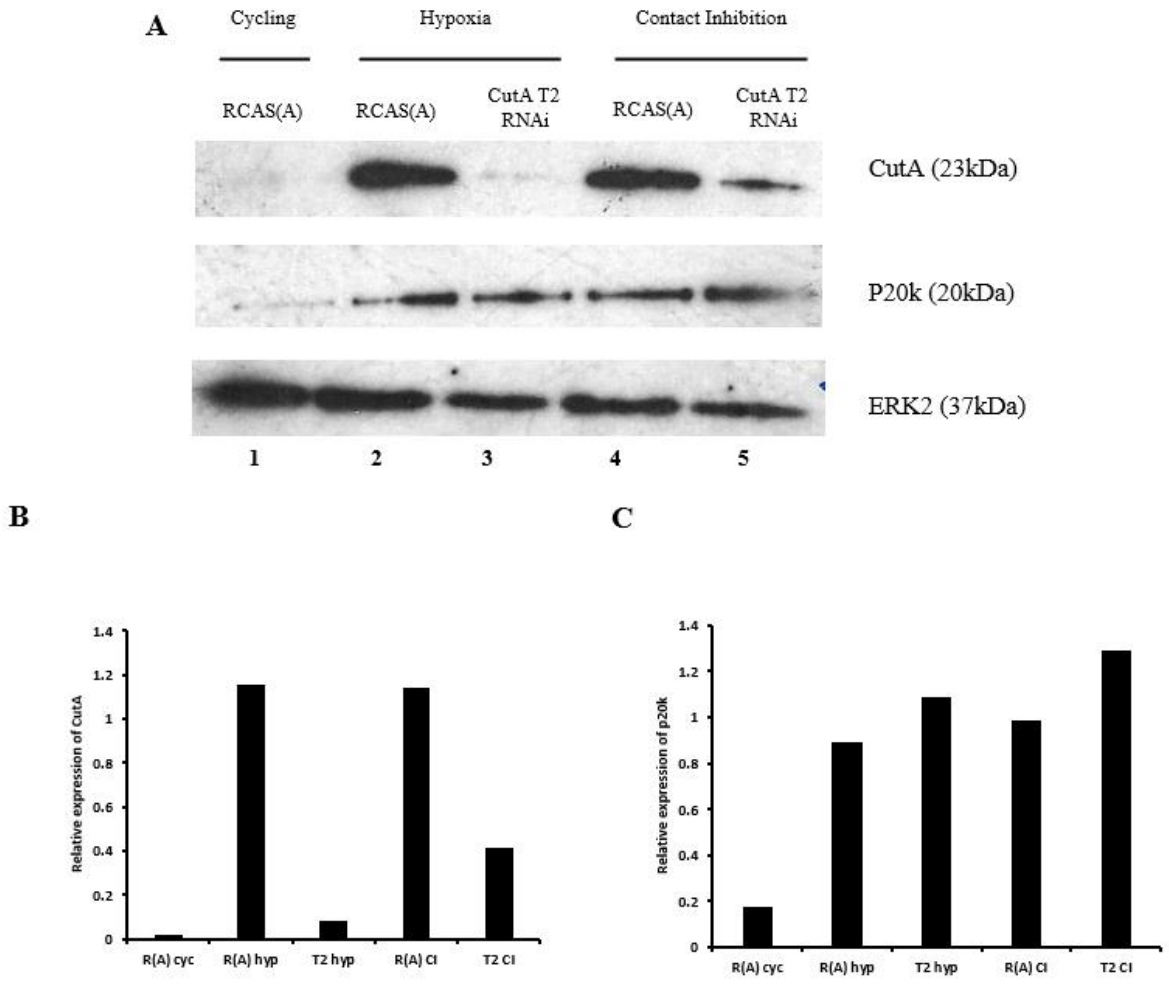

Figure 11. Downregulating *cutA* expression in quiescent CEF. *cutA* T2 shRNA was used to conduct RNA interference (RNAi) to downregulate *cutA* expression in quiescent CEF. A) Western blot analysis confirming successful downregulation of *cutA* expression in response to conditions that induce quiescence (lane 3, 5). RCASBP vector transfected into CEF to use as control to negate any confounding effects the vector might have on expression levels (lane 2, 4). Normoxic CEF used as positive control for absence of *cutA* expression. Blot was also probed with p20k to confirm CEF were experiencing quiescence as well as investigating effect on expression level relative to *cutA*. Basal expression of *cutA* seen in normoxic samples, attributed to uneven

distribution of CEF in tissue culturing plate. B) Quantification analysis of Western blot looking at the downregulation of *cutA* expression, with greater downregulation observed in response to hypoxia than in response to contact inhibition. C) Quantification analysis of Western Blot looking at p20k expression, with hypoxia and contact inhibition samples exhibiting relatively similar expression levels regardless of *cutA* expression. Basal expression of p20k seen in normoxic samples, attributed to uneven distribution of CEF in tissue culturing plate.

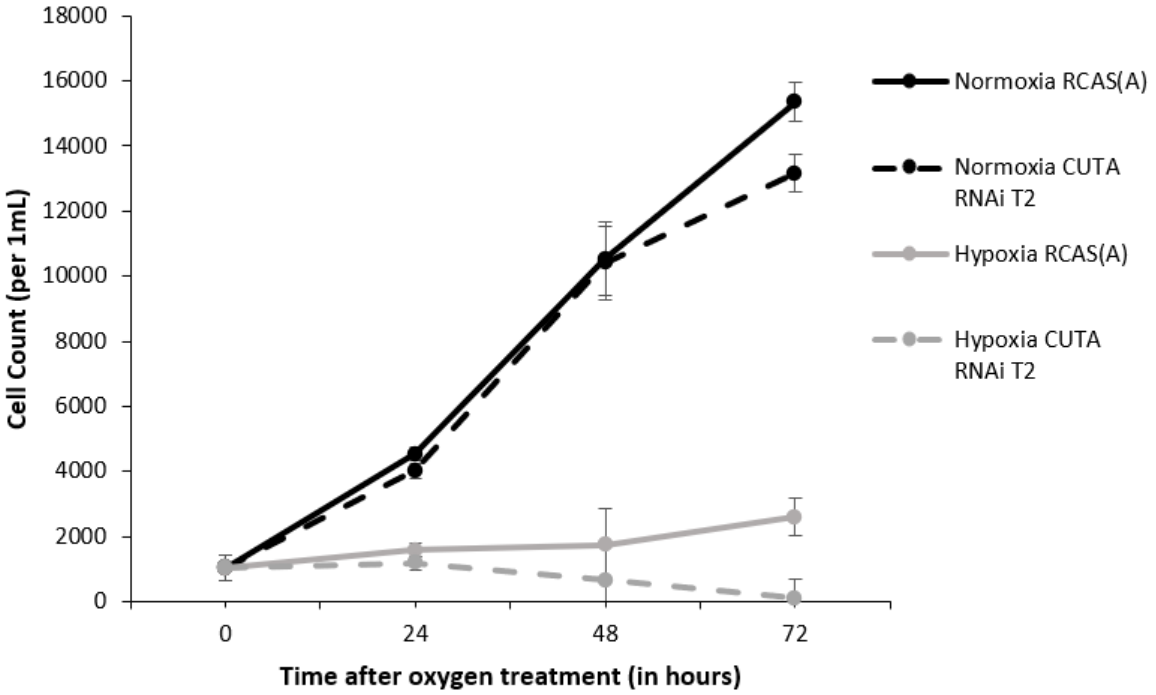

Figure 12. *cutA* expression affects cell proliferation of CEF in quiescence. A proliferation assay comparing cell population count of RCAS(A) control cells and *cutA* T2 shRNA cells in conditions of hypoxia (1.8% O2) and normoxia at 0, 24, 48, and 72 hours. Statistical significance denoted by asterisks, where * represents $p<0.05$, and ** represents $p<0.01$. Error bars indicate the standard deviation in cell population measured in quadruplicate.

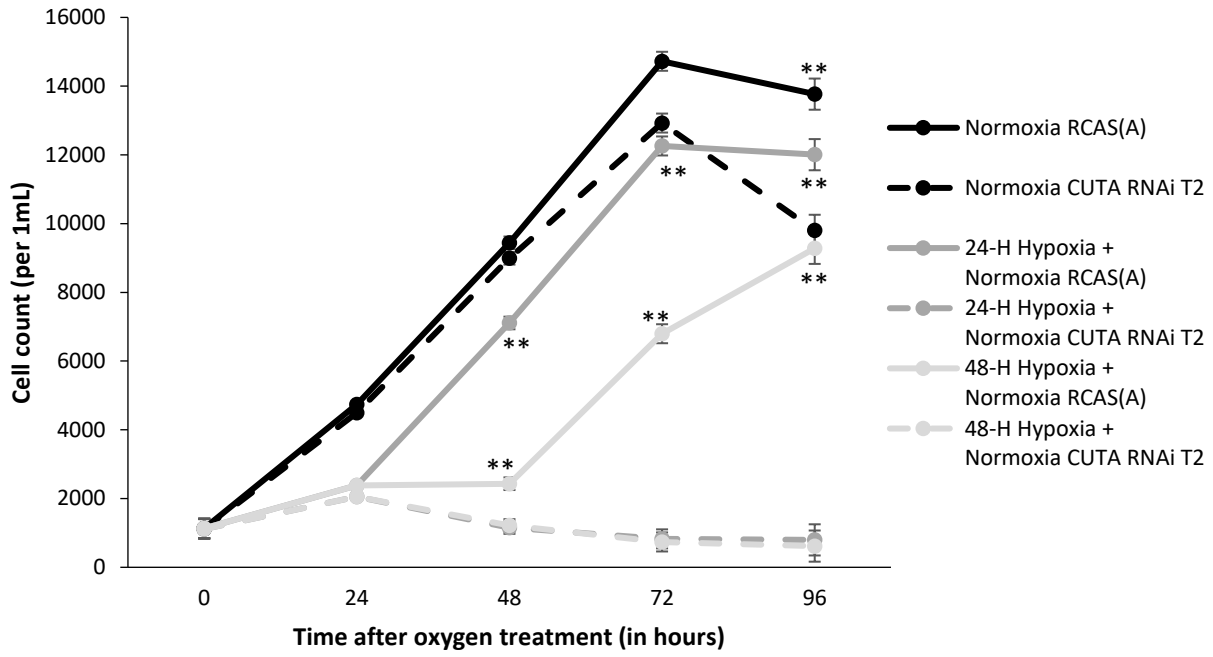

Figure 13. *cutA* expression affects CEF exit from quiescence. A proliferation assay comparing cell population count of RCAS(A) control cells and *cutA* T2 shRNA cells in conditions of hypoxia (1.8% O2) and upon re-establishment of normoxia to investigate effect of *cutA* expression on CEF being able to return to proliferating upon returning to normoxia. Both cell populations were exposed to hypoxia for 24 and 48 hours before being returned to normoxia for a cumulative total of 96 hours post 0-hour count. RCAS(A) and *cutA* T2 shRNA cell counts were taken in hypoxia and normoxia at all time points as control. Statistical significance denoted by asterisks, where * represents $p<0.05$, and ** represents $p<0.01$. Error bars indicate the standard deviation in cell population measured in quadruplicate.

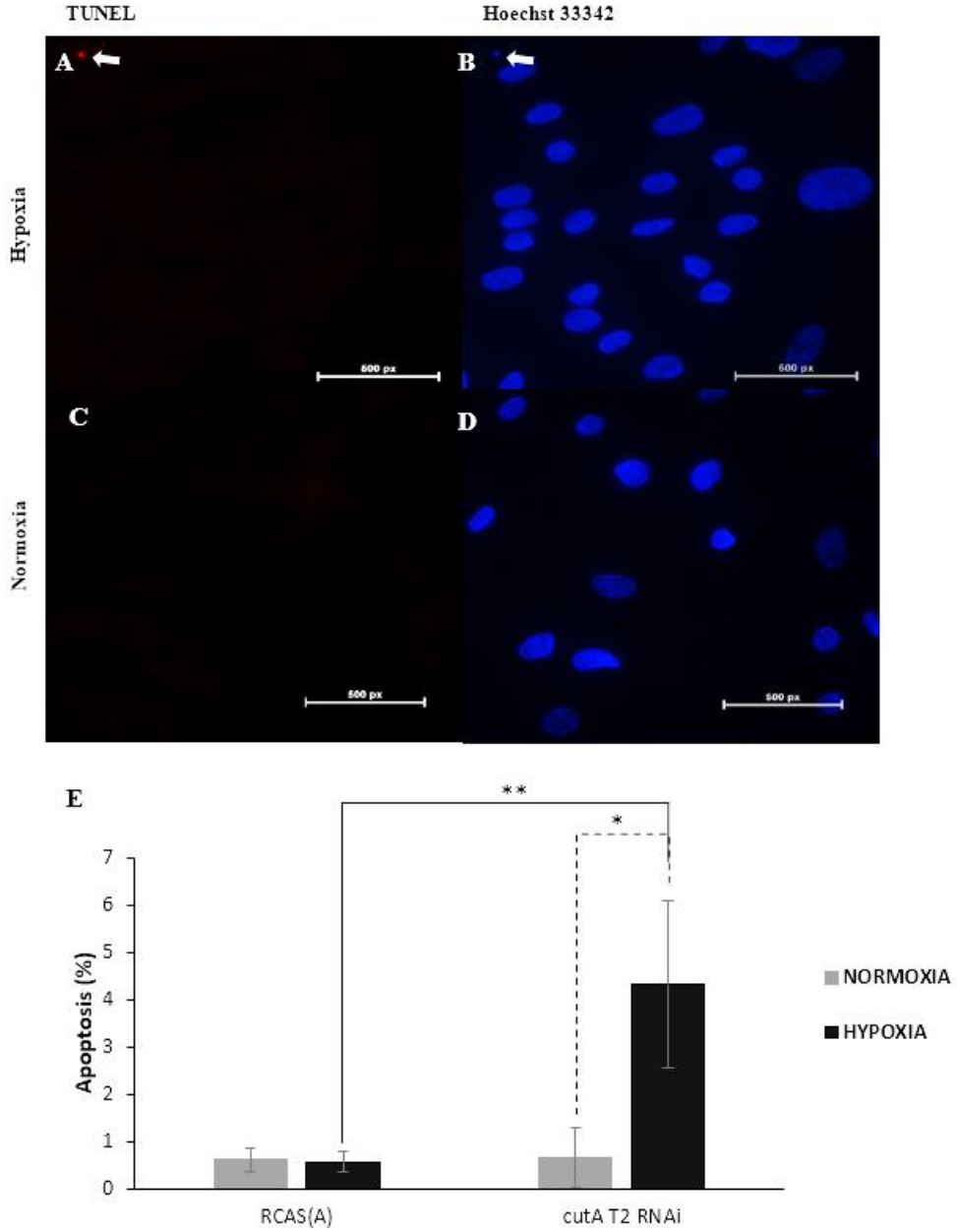

Figure 14: Fluorescent staining with TUNEL assay. A-B) CEF transfected with group A retroviral vector only (RCASBP(A)), and C-D)CEF transfected with group A retroviral vector expressing a shRNA for *cutA* (RCASBP(A) – T2 *cutA* RNAi) were incubated in normoxic (21% O2) or hypoxic (1.8% O2) conditions for 24 hours. The left panels show CEF stained with TdT and TMR red fluorescent labelled dUTP, wherein the white arrows indicate TUNEL-positive (apoptotic) cells. The right panels show CEF nuclei stained with Hoechst 33342, wherein the

white arrows indicate nuclei undergoing chromatin condensation and nuclear fragmentation. E) Quantification of apoptosis in RCASBP(A) and RCASBP(A) – T2 *cutA* RNAi in conditions of normoxia or hypoxia. Error bars represent the mean standard deviation of the levels of apoptosis per 2000 cells, measured in quadruplicate.

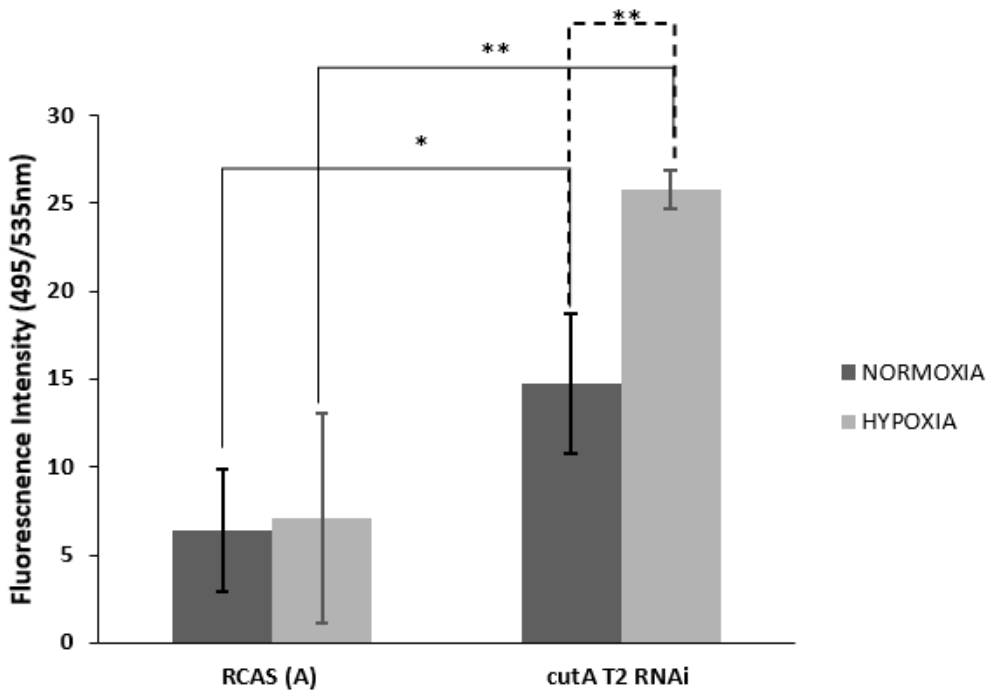

Figure 15: Quantification of cellular reactive oxygen species (ROS) in quiescent CEF with DCFDA ROS assay. CEF transfected with a group A retroviral vector alone and CEF transfected with a group A retroviral vector expressing *cutA* T2 shRNA, were incubated in normoxic (21% O2) and hypoxic (1.8% O2) conditions for 24 hours. Error bars represent the mean standard deviation of the fluorescence intensity measured in quadruplicate. One-way ANOVA tests were conducted to compare fluorescence intensity within and across cell populations. Asterisks indicate significant difference between samples being compared, with * indicating $p<0.05$ and ** indicating $p<0.01$.

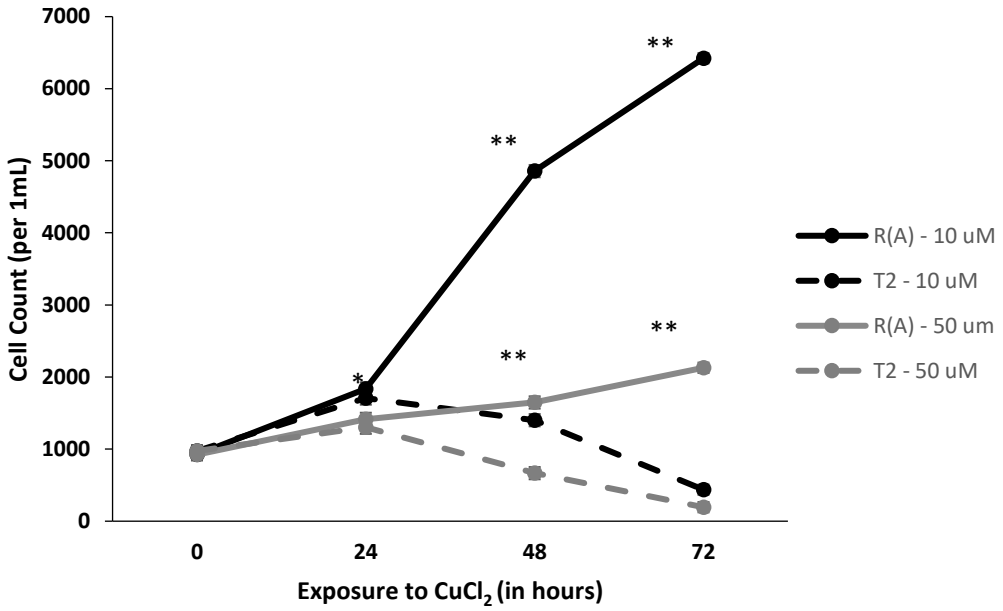

Figure 16. $CuCl_2$ dosage curve in CEF. A proliferation assay comparing cell population count of RCAS(A) control cells and *cutA* T2 shRNA cells in response to metal salt ($CuCl_2$) treatment of two different concentrations (10 µM, 50µM) at 0, 24, 48, and 72 hours. Statistical significance denoted by asterisks, where * represents $p<0.05$, and ** represents $p<0.01$. Error bars indicate the standard deviation in cell population measured in quadruplicate.

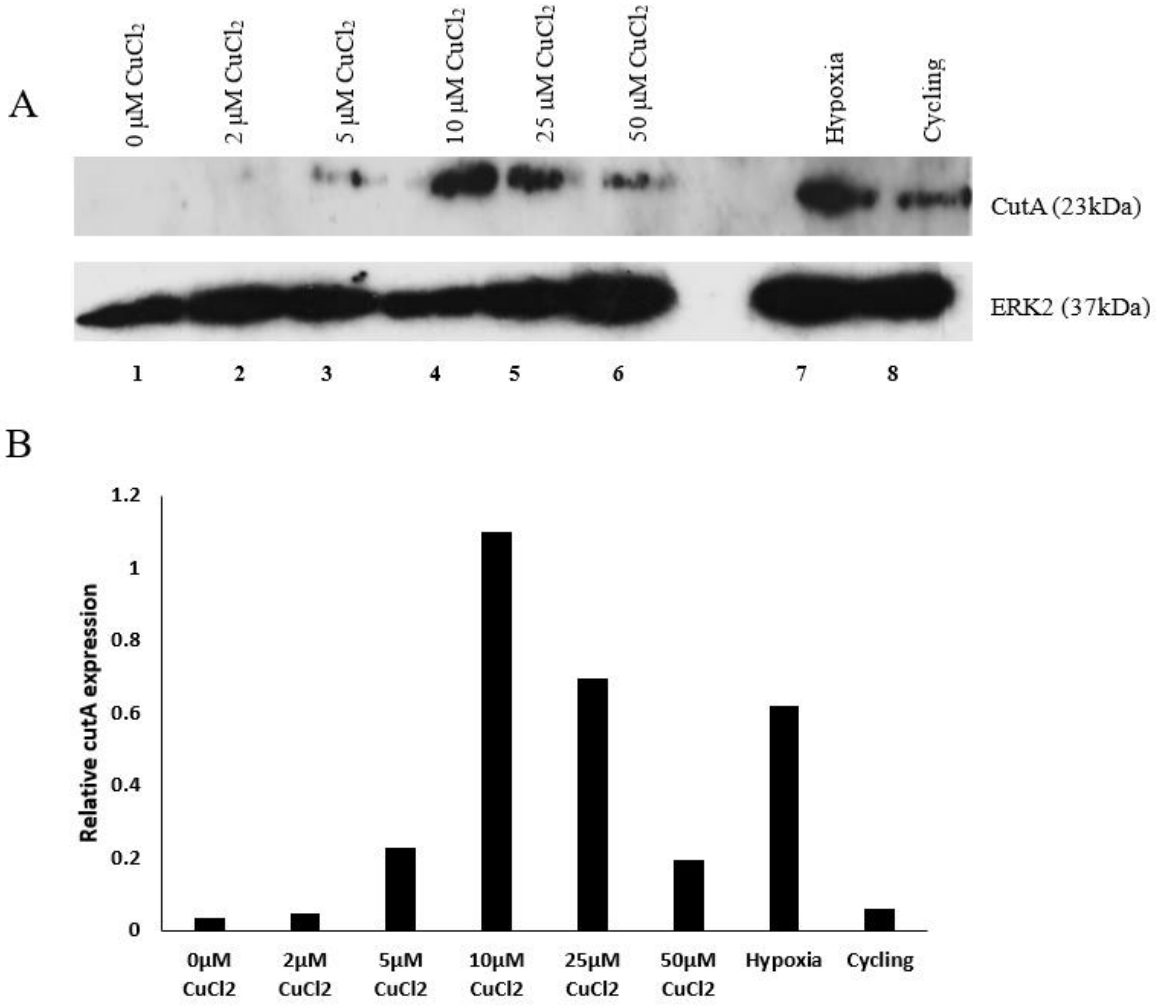

Figure 17. *cutA* expression induction at different $CuCl_2$ concentrations. Western blot analysis showing *cutA* expression induction in response to different concentrations of $CuCl_2$ (lane 1-6). Hypoxia treated CEF (lane 7) used as positive control for induction of *cutA* expression and cycling CEF (lane 8) used as negative control for absence of *cutA* expression. B) Quantification analysis of Western blot looking at *cutA* expression induction in response to different concentrations of $CuCl_2$.

Discussion:

1. Characterization of *cutA* expression and intra-cellular localization in CEF

i. *cutA* is induced by oxygen limiting – hypoxia or contact inhibition – conditions that induce quiescence in CEF.

Gene profiling studies showed that *cutA* is upregulated 50-fold at high cell densities, i. e., where cells are experiencing contact inhibition, a condition characterized by hypoxia (Erb et al., 2016). Both contact inhibition and hypoxia are environmental conditions that induce cellular quiescence, i.e., reversible growth arrest (Erb et al., 2016). This suggested that *cutA* has potential to be a GAS gene. Western blot analysis confirmed that conditions that induce quiescence, i.e., hypoxia and contact inhibition, successfully induce expression of *cutA*. It was noted that *cutA* expression levels were highest following 24-hours of limited oxygen treatment (~1.8% O_2) relative to the expression levels seen in response to maximal confluence. Confirmation of *cutA* expression in quiescent CEF prove that it is a GAS gene, providing further avenues of exploration when investigating its function in CEF. Previously characterized GAS genes, such as p20K and FABP4, both of which have expression pattern similar to *cutA* in response to hypoxia and in response contact inhibition, play a role in promoting cell survival in quiescence in response to hypoxia. Since they share similar expression patterns, investigations to determine if *cutA* also has a pro-survival function, were necessary. To optimize such studies, it was necessary to determine optimal treatment time that induces maximal expression of *cutA.*

Follow-up studies investigating induction time of *cutA* revealed that in response to hypoxia, it is expressed within 2 hours (Figure 8A-B). Compared to this, p20K takes 6 hours to be induced, while FABP4 takes 12 hours, suggesting that *cutA* is one of the first GAS genes to be induced in response to a cell entering quiescence (Erb et al., 2016; Donders, MSc. Thesis, 2020). Maximal

expression of *cutA* is seen at 16 hours in response to hypoxia, with a reduction in accumulation being observed at 30 hours (Figure 8A-B). A similar reduction in accumulation was noted for p20K at 30 hours (Erb et al., 2016). In response to metal addition, *cutA* expression was induced at 4 hours, with maximal expression seen at 32 hours, and reduction in accumulation occurring at 40 hours and thereafter (Figure 8C-D). Of note here is that in both conditions, *cutA* expression is induced quickly , but it takes longer in response to metal addition to reach peak expression. The reduction in accumulation in response to either condition could be attributed to reduced cell viability, since the overall number of cells expressing the protein would be reduced, or because the cells are starving.

Table 6. MRE motif in *cutA* sequence

In sequence:	1201 ggggcggggc ttccgttgtc ccgccccggt gggcggcggt gtttgggggа tgagcggggc 1261 ggtgggatga gagagttgtc tgtaaaatca tagaattgct cagtttggag aaggccttaa 1321 agatcatcaa gtccaaccgc aaccaaacca tagtgcccta actcacagcc ctctgctgga 1381 tcatggagtg atttgcagtg tgcaagcgtg gggcgggttt gggatctgtg gtggcgtctg 1441 ttgtgctgag ccctgctggg agcacctcgg gtgggggccg gggctgctga ggggcaggca 1501 gtgctcacag gcagtgccac tctgtgcagc aggactgtgt gggccaagca ccccacaccc 1561 catgtggcaa atatggtcag aagtgcagaa gggagacaaa atgtcgttta tttccatctg 1621 cggacagcag ggaaggtacg gattgtatca gtgcccgtgc cgggcagcac ctggcatatg 1681 tctgaagtcg tgacacgttt gaggcccacg gcacatcaca gcattcacag ctctggggca 1741 gttcctgccc aaagcacaaa gccccagagt aagaaaaaaa caccgaatgg tgggaagatg 1801 aaggcaggag gagggggcct gcgctccggc cccgtgctgg gcaggcagga gggtgggctg 1861 gttggactag acggcctcag
MTF-1	TGCGCTC

The quicker onset of *cutA* expression might be due to how it is regulated. While the regulation of both p20K and FABP4 in CEF has been documented, with CEBP/β being responsible for activating the expression of both in concert with various other factors, the regulation of *cutA* in CEF has yet to be characterized (Erb et al., 2016; Donders, MSc. Thesis, 2020). Upon sequence analysis of the upstream genome region of *cutA* in *Gallus gallus,* i.e., chicken, a short DNA sequence motif was found, that was annotated as being a metal response element (MRE)(Table 6). MREs are often found in the upstream regulatory sequences of other heavy metal responsive genes such as *metallothionein* (MT) genes (Murphy et al., 2008; Günther, Lindert & Schaffner, 2012) . MT proteins are known to protect against heavy metal and oxidative stress induced cellular damage and subsequent apoptosis (Andrews, 2000; Shimoda et al., 2003; Murphy, 2004). Studies have found that in mammals, in hypoxia induced transcription of MT genes MRE-binding transcription factor 1 (MTF-1) is recruited to the promoter, which in turn recruits different co-activators and other transcription factors to induce target gene expression (Figure 18) (Murphy, 2004; Murphy et al., 2008; Günther, Lindert & Schaffner, 2012). MTF-1 is known to help protect against oxidative stress and hypoxia, as wells as in homeostasis of heavy metals (Murphy et al., 1999; Green et al., 2001; Andrews, 2000; Murphy, 2004; Murphy et al., 2005; Günther, Lindert & Schaffner, 2012; Dubé et al., 2014). Subsequent studies have found that hypoxia-inducible transcription factor-1α (HIF-1 α) is necessary for the hypoxia-induced recruitment of MTF-1 (Murphy, 2004; Murphy et al., 2008). Subsequent investigations show that MTF-1 and HIF-1α are both recruited to MT gene promoters, with HIF-1α interacting with MTF-1, acting as a coactivator of MT gene transcription, during hypoxia (Murphy et al., 2008).

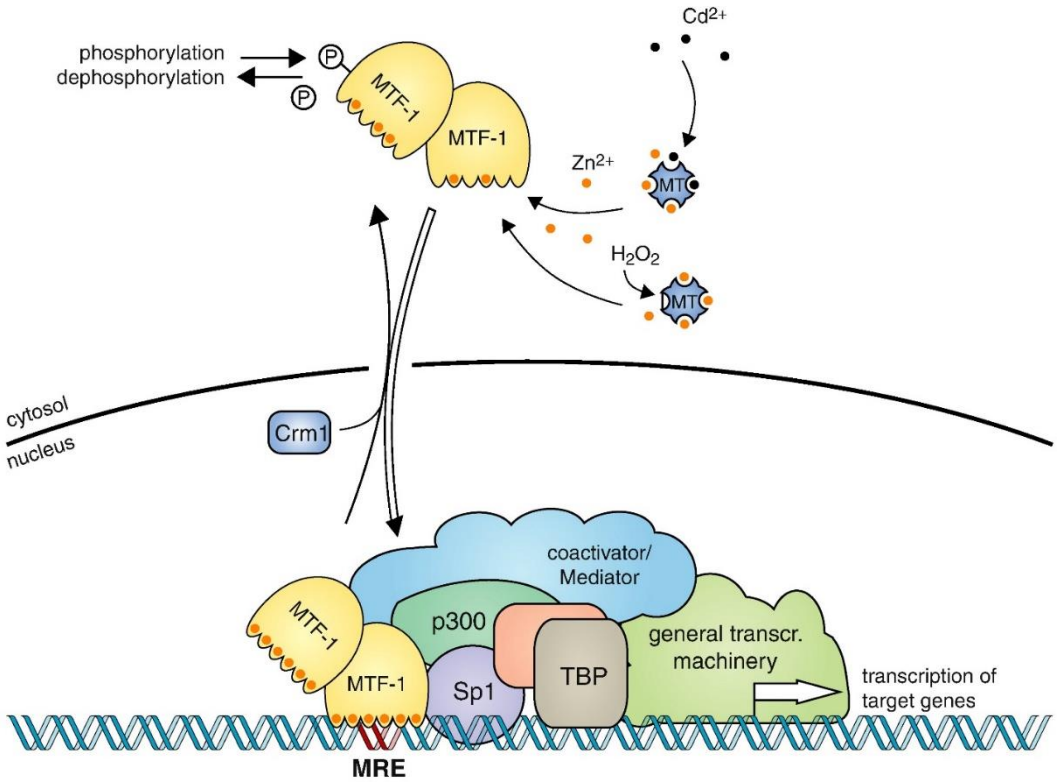

Figure 18. Regulation of mammalian MTF-1. In normal conditions, MTF-1 shuttles between cytoplasm and nucleus, with the interaction of MTF-1 with Crm1 most likely mediating the export. MTF-1 is activated directly by zinc, or indirectly by the release of zinc from metallothioneins due to cadmium load or oxidative stress. In additions, its activity is modulated by phosphorylation. MTF-1, in response to zinc binding, shuttles to the nucleus, binding to its cognate DNA motif, MRE, where it interacts with other transcription factors (e.g., Sp1) and coactivators (e.g., p300) to induce target gene expression (Adapted from Gunther, Lindert & Schaffner, 2012).

Given that *cutA* is highly conserved across species, the presence of the MRE motif, as well as considering the stimuli that induce its expression, it can be proposed that in response to hypoxia, HIF-1α promotes the recruitment of MTF-1, and in concert with it, activates the transcription of *cutA.* Studies have shown the mitochondrial ROS is produced in response to hypoxia, which work to inhibit prolyl hydroxylases (PHDs) activity. PHDs hydroxylate HIFα subunits at the prolines,

which tags them to be recognized by the von Hippel Lindau (VHL) tumor suppressor. This leads to the ubiquitination and degradation of HIFα. In hypoxia, the inhibition of the PHDs allow for HIFα subunits to be stabilized, resulting in HIFα-mediated transcription (Figure 19) (Hamanaka & Chandel, 2009). It has been seen in other studies that stabilization of HIF-1α promotes MTF-1 recruitment to the MRE, where in conjunction with HIF-1α, it activates the transcription of the target genes, which in the proposed mechanism, is *cutA* (Figure 20). In response to metal addition, the same proposed mechanism would apply, since studies have shown that high doses of Cu exposure can cause oxidative stress which results in increased levels of ROS (Liu et al., 2020) (Figure 18). Further studies investigating the promoter activity of *cutA* are necessary to determine whether the regulation of *cutA* occurs in a manner to what has been proposed or if there is a different mechanism at play.

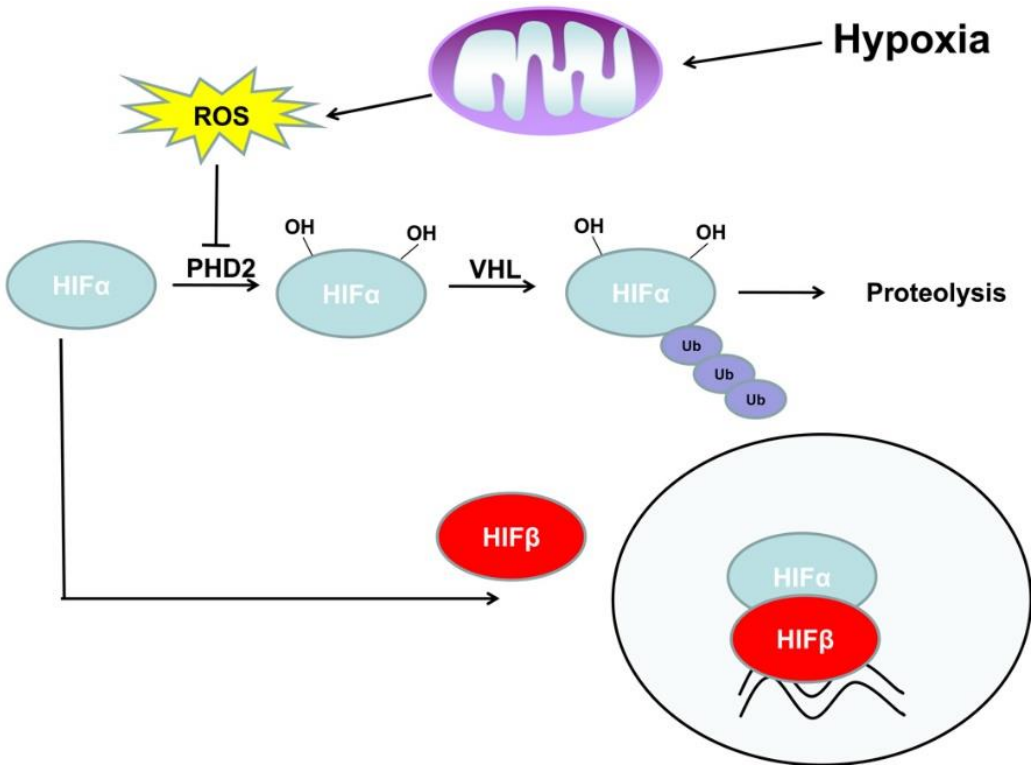

Figure 19. Mitochondrial ROS promote HIFα stabilization. In normoxia, HIFα subunits are hydroxylated by PHDs at prolines, tagging them for ubiquitination by VHL, and subsequent degradation via proteolysis. In hypoxia, mitochondrial ROS inhibit PHD activity, allowing for the stabilization of HIFα subunits and HIFα-mediated transcription of target genes (Adapted from Hamanaka & Chandel, 2009).

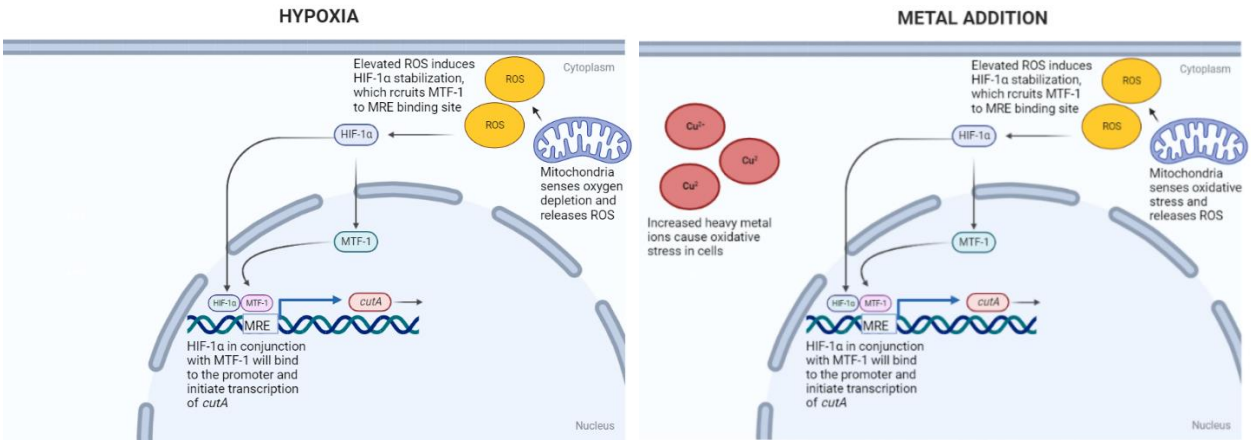

Figure 20. Proposed mechanism of *cutA* activation in CEF. In response to hypoxia, or addition of heavy metals, oxidative stress is exerted on the cell. The mitochondria sensing the oxidative stress, release ROS into the cytosol. Increased mitochondrial ROS accumulation stabilizes HIF-1α by inhibiting the activity of PHD, which will then recruit MTF-1 to its putative binding site, MRE, in the *cutA* promoter. It will then interact with MTF-1, forming a transcriptional complex, to initiate the transcription of *cutA*.

ii. *cutA* is induced in response to $CuCl_2$ treatment and requires prolonged treatment exposure to reach maximal expression.

cutA has also been implicated in metal sensing and tolerance, with varied speculations having been put forth about its specific role in relation to metal salts (Fong, Camakaris, & Lee, 1995; Selim et al., 2021). In *E. coli*, characterization of the crystal structure of *cutA* revealed the presence of mercury ions bound to the protein. Other studies have shown copper binding to *cutA* in *E. coli* and have also shown the increased metal sensitivity of cells in *E. coli* in the absence of *cutA* (Arnesano et al., 2003; Fong, Camakaris, & Lee, 1995) (Figure 21). Based on these, it was proposed that in bacteria, CutA binds copper, shuttling it out of the cell, and hence maintaining copper homeostasis. Based on what was seen in *E. coli*, investigations were conducted to determine

induction of *cutA* in response to metal addition. Western blot analyses confirmed expression induction in response to metal addition (here, $CuCl_2$ treatment) (Figure 7). To determine the optimal conditions for *cutA* induction, it was necessary to determine the ideal concentration of $CuCl_2$ as well as the optimal treatment time, which resulted in maximal expression of *cutA*. Western blot analyses testing different concentrations confirmed that 10 µM $CuCl_2$ resulted in maximal expression in CEF (Figure 16). Investigation into optimal $CuCl_2$ treatment time revealed that CutA is induced as early as 4 hours, with maximal expression seen at 32 hours, double the time it takes in response to hypoxia, with a reduction in accumulation being observed at 40 hours and after (Figure 8). The longer duration of time required to reach maximal expression of *cutA* following $CuCl_2$ treatment could be attributed to the cell responding to increased accumulation of copper ions within the cell. This might suggest that, just like in *E. coli*, wherein CutA binding to copper has been observed, in CEF, CutA binds copper ions to reduce excess copper and prevent cytotoxicity resulting from accumulation of metal ions (Figure 10) (Arnesano et al., 2003; Fong, Camakaris, & Lee, 1995).

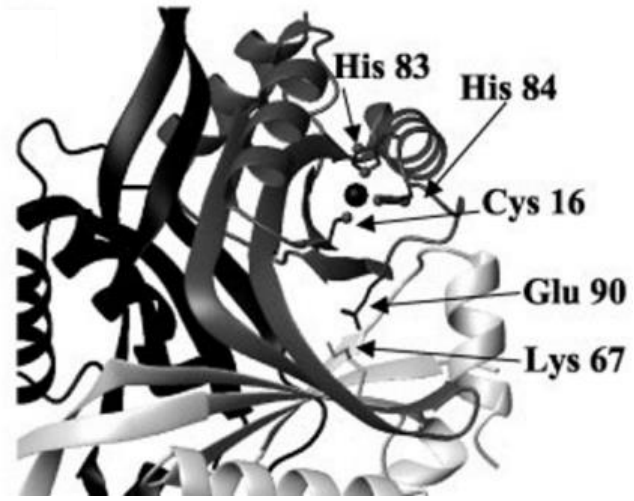

Figure 21. Crystal structure modelling of Cu(II) binding site on *E. coli* CutA1 homolog. The potential binding site is denoted by the black sphere, with the potential residues labelled (Arnesano et al., 2003).

iii. *cutA* is found to localize in the cytoplasm of CEF, closer to the periphery, near the cell membrane

To better understand its function in CEF, it was important to determine the intracellular localization of *cutA* in response to the various conditions that induce its expression. To that effect, immunofluorescence analyses were performed which showed that *cutA* is seen expressed in response to hypoxia, and in response to $CuCl_2$ treatment, confirming our Western blot analyses. Overall, the immunofluorescence analyses provided further evidence supporting that *cutA* is a GAS gene and has a role in response to metal addition.

In response to hypoxia, CutA was seen to localize in the periphery of the cell and in small round clusters within the cytosol. This is very different from what is known of the localization of CEBP/β regulated GAS genes, namely p20K, which are seen expressed in the endomembrane system in CEF (Bedard et al., 1987). The difference in intracellular localization provides further proof that

cutA, while sharing similar expression pattern with p20K in response to environmental conditions that induce quiescence, may be regulated differently and might be part of a different protein cascade or pathway than p20K. To further investigate the subcellular localization of CutA in quiescent CEF, more immunofluorescence analyses using biomarkers for cellular organelles are necessary. A study by Yang and colleagues (2009) showed subcellular localization of a *cutA* isoform, CUTA2. They performed immunofluorescence analysis on HeLa overexpressing CUTA2 isoform and found it to be concentrated in the perinuclear region but with predominant co-localization with mitochondria. This suggested that CUTA2 was predominantly subcellularly localized to the mitochondria (Yang et al., 2009).

In CEF treated with $CuCl_2$, CutA was seen clustered at the edges of the cell membrane in dense circular formation. In previous studies, CutA has been thought to reduce excess copper in cells by binding copper ions – an interaction that has been seen occurring *in-vitro* with bacterial CutA (Arnesano et al., 2003). It has also been speculated to interact with cell membrane transporters and affect the import and export of copper (Fong, Camakaris, & Lee, 1995; Rensing & Grass, 2003). Another study showed mammalian CutA to be partly contained with the secretory compartment from which it could be released into the medium (Liang et al., 2009). Based on these speculations, and in conjunction with the results obtained from the immunofluorescence analyses, it can be proposed that CutA is responsible for trafficking metal out of cells by binding the ions, hence reducing the cellular concentration of metals to be tolerable. Further studies testing cellular culture medium for *cutA* expression of CEF treated with $CuCl_2$ are required to determine whether CutA is secreted out in response to metal presence. Chevallet et al., (2007) detail various techniques analyzing cell secretomes that could be employed for the aforementioned studies and also provide suggestions to overcome challenges present with current proteomic techniques.

2. Functional characterization of *cutA* in CEF

i. shRNA mediated downregulation of *cutA* allows for the functional characterization and reveals information about its relation to other GAS genes

cutA has been characterized as a GAS gene based on its upregulation in oxygen depleted environmental conditions, such as hypoxia and maximal confluence, that induce cellular quiescence (Figure 7, 9A-F). Despite our understanding of its expression patterns, and localization within CEF, its role in quiescence remains unknown. Development of retroviral shRNA RCASBP vectors targeting *cutA* provide a molecular tool to investigate the effects of *cutA* in quiescent CEF. In line with our previous results that revealed an absence of *cutA* expression in actively proliferating cells, no *cutA* expression was seen in actively proliferating control and *cutA* shRNA CEF (Figure 7, 11A-B). Elevated levels of *cutA* expression were observed in control CEF in oxygen depleted conditions (~1.8% O_2, or maximal confluence), while *cutA* shRNA CEF showed no expression in these conditions (Figure 11A-B). This confirms that *cutA* downregulation can be attained using RCASBP(A)-*cutA* T2 RNAi, providing an effective model to investigate the function of *cutA* in quiescence.

Previous studies have suggested that there is cross-regulation between FABP4 and p20K lipocalin. It has been observed that when either one is downregulated, expression of the other is lost as well (Donders, MSc., 2020) In conjunction with this, investigation into effect on *cutA* expression when p20K is downregulated showed no disruption of *cutA* expression (Moftakhari, et al., in preparation). The question remains as to what effect disrupting *cutA* expression would have on the expression of p20K. Western blot analyses showed no change in p20K induction upon shRNA-mediated downregulation of *cutA* (Figure 11A,C). These results, in conjunction with previous observations about lack of *cutA* expression disruption upon p20K downregulation,

provide more evidence supporting that *cutA* is regulated differently from p20K and is a part of a different pathway, not involving C/EBPβ.

ii. *cutA* promotes survival in quiescent CEF

Quiescence i.e., reversible growth arrest, induces unique gene expression that promotes cell survival by mitigating cellular stressors, and preventing proliferation, while permitting re-entry into the proliferative state upon re-establishment of optimal growth conditions. It has been previously established that contact inhibited cells experience hypoxia in culture, indicating that some GAS genes are regulated indirectly by hypoxia, wherein induction of quiescence by hypoxia causes gene expression to be induced (Erb et al., 2016). Gene profiling studies identified *cutA* as one such gene, with subsequent investigations into its expression pattern, confirming the same at the protein level (Figure 7). Despite being recognized as having various functions across different species, its specific role in quiescence remains unidentified. In bacteria, like *E. coli*, *cutA* homologs have been shown to be involved in heavy metal binding, with binding of *cutA* to metal ions such as Cu(II) being confirmed (Figure 21) (Arnesano et al., 2003; Fong, Camkaris & Lee, 1995). In humans, it has been proposed that *cutA* is involved in anchoring AChE in human neuronal cell membrane (Hou et al., 2015; Arnesano et al., 2003). Aberrant *cutA* expressing cells have been shown to gain sensitivity to heavy metals, and other subsequent studies have proposed that *cutA* might be involved in mitigating heavy metal accumulation to promote cell survival, linking its function in heavy metal tolerance to its involvement in anchoring AchE in human neuronal cells, since heavy metals are involved in neurological disorder pathologies (Arnesano et al., 2003). These findings suggest that *cutA* does promote cell survival by mitigating cellular stressors, which in this case would be excess heavy metal accumulation. Preliminary investigations done to assess effect

of different concentrations of $CuCl_2$ treatment on cell viability revealed that *cutA* expression has a pro-survival role, as cell populations with aberrant *cutA* expression, when treated with $CuCl_2$, exhibited a loss of cell viability (Figure 17, data not shown).

Evaluating the effect of aberrant *cutA* expression on cell population in hypoxia revealed that number of *cutA* shRNA expressing cells decrease unlike the control cells (Figure 12). In normoxia, no difference was observed between either cell population. This suggests that *cutA* expression promotes survival in quiescence induced in response to hypoxia. It was also noted that overall, cells incubated in hypoxic conditions had a lower proliferation rate than seen in cells incubated in normoxia, showing that oxygen availability impacts cells proliferation. This is expected as cell division is a metabolically taxing process, requiring oxygen for aerobic respiration to fuel it (Kalucka et al., 2015).

An extended version of the experiment done to evaluate the effect of *cutA* expression on CEF upon re-establishment of optimal growth conditions revealed that CEF with aberrant *cutA* expression, in conditions of hypoxia, were unable to return to a proliferative state. Comparatively, control cells returned to proliferating normally upon re-establishment of normoxic conditions, which confirms that *cutA* acts as a GAS gene, and can permit re-entry into a proliferative state when normal growth conditions are restored. The findings also serve to confirm that cells are entering growth arrest and that it is reversible, as evidenced by maintenance of control cell population numbers while in hypoxia, and the increased numbers, attributed to re-entry into active proliferative state, upon restoration of normoxia (Coller, 2011).

Subsequently, TUNEL assays were conducted to ascertain whether the reduced cell population noted in hypoxia for CEF with *cutA* downregulation was caused by reduced cell viability attributable to apoptosis. Apoptosis, first termed as such by Kerr, Wylie, & Currie (1972), occurs

during development and aging, acting as a homeostatic mechanism of maintaining cell populations. It also acts as an anti-tumorigenic defense in response to cell damage resulting from disease or toxic agents, removing damaged cells to maintain tissue integrity (Norbury & Hickson, 2001; Elmore, 2007). Hypoxia can induce apoptosis via various mechanisms. One such mechanism is high induction of pro-apoptotic proteins like BNIP3 by HIF-1, which in turn inhibit anti-apoptotic proteins like Bcl2/Bcl-xl. This in concert with the stabilisation of p53 by HIF-1 activates the signalling cascade resulting in cellular apoptosis (Reynolds, Rockwell & Glazer, 1996; Gross et al., 1999; Guo et al., 2001; Greijer & Wall, 2004). A complex equilibrium between anti- and pro-apoptotic factors eventually decides cell fate in hypoxia (Figure 22). Apoptosis is morphologically characterized by pyknosis, which is the irreversible condensation of chromatin.

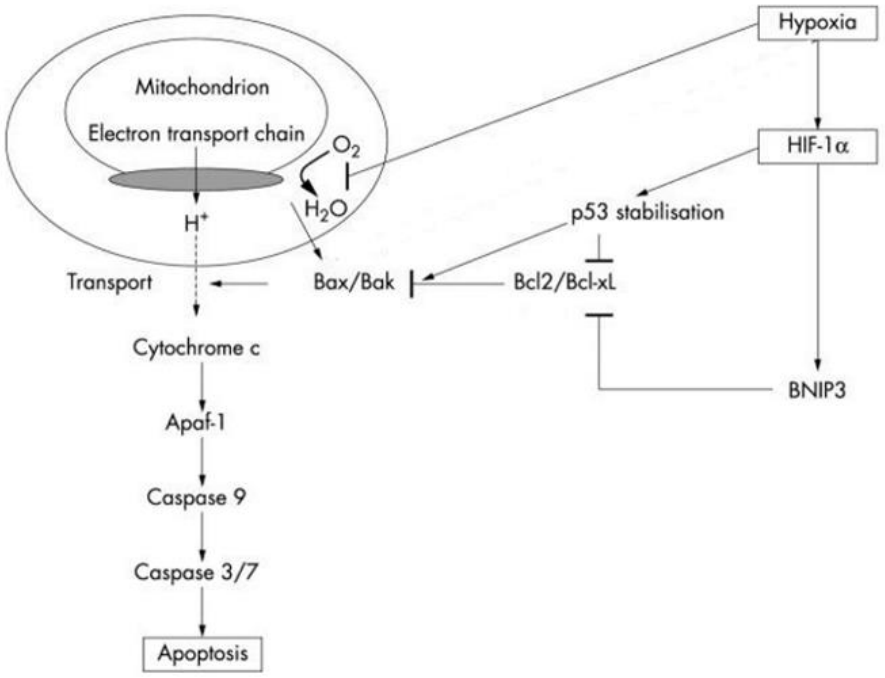

Figure 22. Schematic representation of apoptosis signalling cascades induced by hypoxia (Adapted from Greijer & Wall, 2004)

An increased incidence of apoptosis was observed in samples expressing the *cutA* shRNA in comparison to control samples and samples in normoxia (Figure 13). Typically, as seen in the control samples, CEF show negligible incidence of apoptosis after 24-30 hours of exposure to hypoxia, which is indicative of their ability to adapt to/tolerate low oxygen environments. These findings are complemented by the overall increasing trend, albeit occurring at a slower rate than in normoxia, seen in the control cell populations in hypoxia. Overall, the findings indicate that *cutA* preserves cell viability in hypoxia, potentially by promoting adaptation to the oxygen depleted environment or by promoting the induction of anti-apoptotic factors such as inhibitor of apoptosis protein (IAP-2), which previous studies have shown to be induced by the hypoxia induced transcription factor nuclear factor κB (NF-κB) (Dong et al., 2003).

iii. Aberrant *cutA* expression shows increased ROS accumulation in quiescent CEF

The increased production and accumulation of cellular ROS is often associated with lipid peroxidation, which involves the formation of lipid radicals that can initiate free radical attacks on the surrounding lipids, resulting in a cascade that damages lipid membrane integrity (Yin, Xu & Porter, 2011; Juan et al., 2021). Increased ROS production during prolonged periods of hypoxia is mostly mitochondria-mediated as it senses oxygen levels and will release ROS into the cytosol to stabilize HIF-1α and HIF-2α. This in turn will prime the cellular response to oxygen deprivation (Chandel et al., 1998; Guzy et al., 2005). shRNA-mediated downregulation of *cutA* caused a significantly elevated level of ROS accumulation in hypoxia when compared to control cells in hypoxia (~3.3 fold) (Figure 23). These findings, in concert with the findings of the TUNEL assay and the proliferation assay suggest that *cutA* contributes to mitigating ROS accumulation to prevent apoptosis and promote cell survival in hypoxia. Increased ROS accumulation is associated

with lipid peroxidation, wherein lipid peroxides, the products of lipid peroxidation, induce apoptosis (Figure 23) (Su et al., 2019). Therefore, *cutA* being able to mitigate the accumulation of ROS to levels that cells can tolerate might be how it helps maintain cell viability. Further investigation is required to confirm whether the increased accumulation of ROS is resulting in formation of lipid radicals that initiate the chain reaction of lipid peroxidation, which can be determined using a malondialdehyde (MDA) colorimetric assay. Whether or not this pro-survival function is associated with metal binding remains to be investigated.

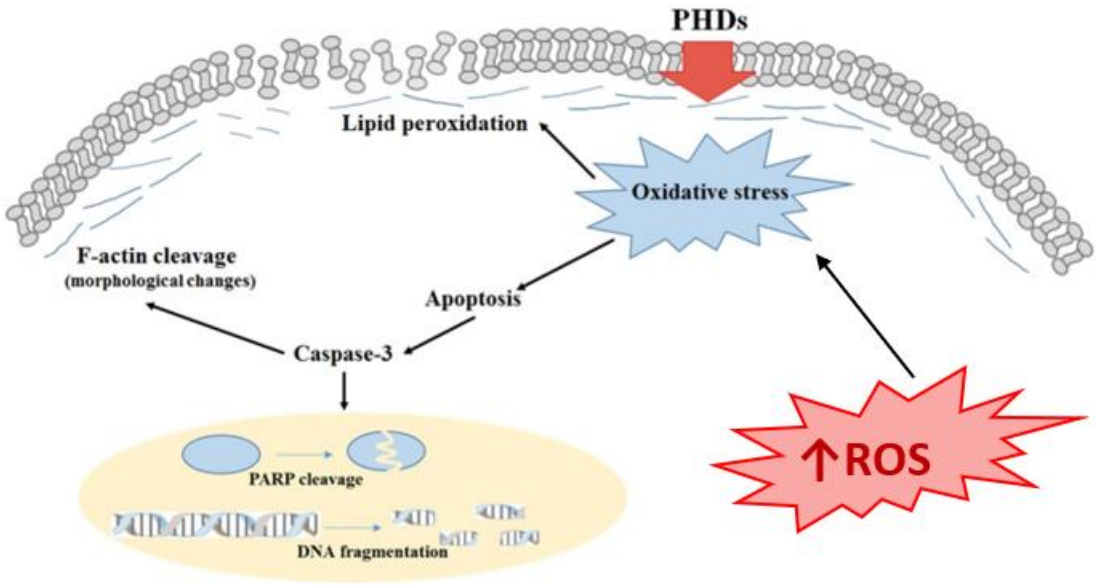

Figure 21: Elevated ROS accumulation leads to apoptosis. Increased ROS accumulation in cells results in oxidative stress being exerted, which results in lipid peroxidation chain reaction to be initiated. The increase in cellular lipid peroxidation augments mitochondrial membrane permeability, in turn causing the release of cytochrome c, which activates executive caspases, inducing apoptosis (Adapted from Środa-Pomianek et al., 2018).

Conclusion and Future Directions:

In summary, this study successfully characterized the expression pattern of *cutA*, showing that it is induced in response to oxygen-depleted (hypoxia, contact inhibition) conditions, and in response to heavy metal addition. This study also showed that *cutA* expression is induced very quickly in response to oxygen depletion as well as metal addition, with the latter requiring a more prolonged exposure to induce peak expression. Sequence analysis of the gene in *G. gallus* revealed the presence of an MRE motif, which is the putative binding region for MTF-1. Based on our findings and previous studies, it can be proposed that in response to hypoxia, HIF-1α is induced, which recruits MTF-1 to its putative binding site, MRE, in the *cutA* promoter. Then, interacting with MTF-1, HIF-1α acts as a co-activator, and initiates the transcription of *cutA*. Further investigations analysing the promoter region of *cutA* are required to confirm if MTF-1 binds to the MRE and whether MTF-1 and HIF-1α are both recruited to the promoter in response to hypoxia. To investigate binding of MTF-1 to the promoter, chromatin immunoprecipitation studies are necessary, along with co-immunoprecipitation studies to investigate MTF-1 and HIF-1α interaction.

Subsequently, intracellular localization of CutA in response to hypoxia was characterized to be different from p20K, which localizes to the endomembrane system, whereas CutA localized predominantly perinuclearly and closer to the periphery, near the cellular membrane. Similar localization pattern was seen for CutA in response to metal addition. Previous studies investigating subcellular localization of human CUTA2 isoform has shown predominant localization to the mitochondria. To investigate subcellular localization of CutA in CEF in response to oxygen depletion and metal addition, co-localization assays using organelle biomarkers are necessary.

Pro-survival function of *cutA* in quiescent CEF was confirmed, with aberrant *cutA* expressing CEF showing reduced cell population numbers in hypoxia compared to control. It was also seen that control CEF were able to return to a proliferative state upon restoration of normoxic conditions, while CEF expressing the *cutA* shRNA couldn't. TUNEL assay and ROS accumulation analyses provided insight into how *cutA* might be able to promote cell survival in hypoxia induced quiescent CEF. Increased apoptosis and ROS accumulation in CEF expressing *cutA* shRNA in concert with the reducing cell population of the same in hypoxia suggest that CutA might be responsible for mitigating ROS accumulation levels to be tolerable by cells, which in turn reduces level of apoptosis. Lastly, the experimental findings in conjunction with previous studies and the presence of the MRE motif in the promoter region, which was revealed upon sequence analysis of the upstream *cutA* genomic region, shed light on a potential mechanism by which *cutA* is regulated and acts to promote cell survival. Future investigations are necessary to determine if the MTF-1 is actually able to bind to the MRE motif present. It is also necessary to determine if there are co-activators or upstream regulators that modulate this interaction.

Overall, this study has provided insight into the expression and potential function and regulation of a GAS gene that is not regulated by C/EBPβ, revealing the potential for a different signalling cascade being required for the maintenance of cell homeostasis.

Appendix: Supplemental Figures

References

Alberts, B., Johnson, A., Lewis, J., Raff, M., Roberts, K., & Walter, P. (2002a). An overview of the cell cycle. In *Molecular Biology of the Cell*. Garland Science.

Alberts, B., Johnson, A., Lewis, J., Raff, M., Roberts, K., & Walter, P. (2002b). The mechanics of cell division. In *Molecular Biology of the Cell*. Garland Science.

Andrews G. K. (2000). Regulation of metallothionein gene expression by oxidative stress and metal ions. *Biochemical pharmacology*, *59*(1), 95–104. https://doi.org/10.1016/s0006-2952(99)00301-9

Arnesano, F., Banci, L., Benvenuti, M., Bertini, I., Calderone, V., Mangani, S., & Viezzoli, M. S. (2003). The evolutionarily conserved trimeric structure of CutA1 proteins suggests a role in signal transduction. *Journal of Biological Chemistry*, *278*(46), 45999–46006. https://doi.org/10.1074/jbc.M304398200

Ayala, A., Muñoz, M. F., & Argüelles, S. (2014). Lipid peroxidation: Production, metabolism, and signaling mechanisms of malondialdehyde and 4-hydroxy-2-nonenal. In *Oxidative Medicine and Cellular Longevity* (Vol. 2014). Landes Bioscience. https://doi.org/10.1155/2014/360438

Barnum, K. J., & O'Connell, M. J. (2014). Cell cycle regulation by checkpoints. *Methods in Molecular Biology*, *1170*, 29–40. https://doi.org/10.1007/978-1-4939-0888-2_2

Barrera, G. (2012a). Oxidative stress and lipid peroxidation products in cancer progression and therapy. *ISRN Oncology*, *2012*, 1–21. https://doi.org/10.5402/2012/137289

Barth, H., & Kinzel, V. (1995). Epidermal growth factor rapidly impairs activation of p34cdc2 protein kinase in HeLa cells at the G_2-M boundary. *Journal of Cellular Physiology 162*, 44–51. https://doi.org/10.1002/jcp.1041620107

Barth, H., Hoffmann, I., & Kinzel, V. (1996). Radiation with 1 Gy prevents the activation of the mitotic inducers mitosispromoting factor (MPF) and cdc25-C in HeLa cells. *Cancer Research 56*, 2268–2272.

Bédard, P. A., Balk, S. D., Gunther, H. S., Morisi, A., & Erikson, R. L. (1987). Repression of quiescence-specific polypeptides in chicken heart mesenchymal cells transformed by Rous sarcoma virus. *Molecular and cellular biology*, *7*(4), 1450–1458. https://doi.org/10.1128/mcb.7.4.1450

Blagosklonny, M. V. (2011). Cell cycle arrest is not senescence. *Aging*, *3*(2), 94–101. https://doi.org/10.18632/aging.100281

Blagosklonny, M. V., & Pardee, A. B. (2013). The restriction point of the cell cycle. In *Madame Curie Bioscience Database.* Landes Bioscience

Bush A. I. (2000). Metals and neuroscience. *Current opinion in chemical biology*, *4*(2), 184–191. https://doi.org/10.1016/s1367-5931(99)00073-3

Cancedda, F. D., Dozins, B., Rossis, F., Molinas, F., Canceddas, R., Negriil, A., & Ronchitl, S. (1990). The Ch21 protein, developmentally regulated in chick embryo, belongs to the superfamily of lipophilic molecule carrier proteins. *Journal of Biological Chemistry, 265*(31), 19060-19064.

Cancedda, F. D., Malpeli, M., Gentili, C., Di Marzo, V., Bet, P., Carlevaro, M., Cermelli, S., & Cancedda, R. (1996). The developmentally regulated avian Ch21 lipocalin is an

extracellular fatty acid-binding protein. *Journal of Biological Chemistry*, *271*(33), 20163–20169. https://doi.org/10.1074/jbc.271.33.20163

Carmeliet, P., Dor, Y., Herber, J. M., Fukumura, D., Brusselmans, K., Dewerchin, M., Neeman, M., Bono, F., Abramovitch, R., Maxwell, P., Koch, C. J., Ratcliffe, P., Moons, L., Jain, R. K., Collen, D., & Keshet, E. (1998). Role of HIF-1α in hypoxiamediated apoptosis, cell proliferation and tumour angiogenesis. *Nature*, *394*(6692), 485–490. https://doi.org/10.1038/28867

Cermelli, S., Zerega, B., Carlevaro, M., Gentili, C., Thorp, B., Farquharson, C., Cancedda, R., & Cancedda, F.D. (2000). Extracellular fatty acid binding protein (Ex-FABP) modulation by inflammatory agents: "Physiological" acute phase response in endochondral bone formation. *European Journal of Cell Biology*, *79*(3), 155–164. https://doi.org/10.1078/S0171-9335(04)70018-7

Chandel, N. S., Maltepe, E., Goldwasser, E., Mathieu, C. E., Simon, M. C., & Schumacker, P. T. (1998). Mitochondrial reactive oxygen species trigger hypoxia-induced transcription. *Proceedings of the National Academy of Sciences of the United States of America*, *95*(20), 11715–11720. https://doi.org/10.1073/pnas.95.20.11715

Chevallet, M., Diemer, H., Van Dorssealer, A., Villiers, C., & Rabilloud, T. (2007). Toward a better analysis of secreted proteins: the example of the myeloid cells secretome. *Proteomics*, *7*(11), 1757–1770. https://doi.org/10.1002/pmic.200601024

Chi, J. T., Wang, Z., Nuyten, D. S. A., Rodriguez, E. H., Schaner, M. E., Salim, A., Wang, Y., Kristensen, G. B., Helland, Å., Børresen-Dale, A. L., Giaccia, A., Longaker, M. T., Hastie, T., Yang, G. P., van de Vijver, M. J., & Brown, P. O. (2006). Gene expression programs in response to hypoxia: Cell type specificity and prognostic significance in

human cancers. *PLoS Medicine*, *3*(3), 395–409. https://doi.org/10.1371/journal.pmed.0030047

Cho, S., & Hwang, E. S. (2012). Status of mTOR activity may phenotypically differentiate senescence and quiescence. *Molecules and Cells*, *33*(6), 597–604. https://doi.org/10.1007/s10059-012-0042-1

Coller H. A. (2011). Cell biology. The essence of quiescence. *Science (New York, N.Y.)*, *334*(6059), 1074–1075. https://doi.org/10.1126/science.1216242

Coller, H. A., Sang, L., & Roberts, J. M. (2006). A new description of cellular quiescence. *PLoS Biology*, *4*(3), e83. https://doi.org/10.1371/journal.pbio.0040083

Cooper, G. M. (2000). The eukaryotic cell cycle. In *The Cell: A Molecular Approach*. Sinauer Associates.

Correnti, C., Clifton, M. C., Abergel, R. J., Allred, B., Hoette, T. M., Ruiz, M., Cancedda, R., Raymond, K. N., Descalzi, F., & Strong, R. K. (2011). Galline Ex-FABP is an antibacterial siderocalin and a lysophosphatidic acid sensor functioning through dual ligand specificities. *Structure*, *19*(12), 1796–1806. https://doi.org/10.1016/j.str.2011.09.019

Cramer, T., Yamanishi, Y., Clausen, B. E., Förster, I., Pawlinski, R., Mackman, N., Haase, V. H., Jaenisch, R., Corr, M., Nizet, V., Firestein, G. S., Gerber, H. P., Ferrara, N., & Johnson, R. S. (2003). HIF-1α is essential for myeloid cell-mediated inflammation. *Cell*, *112*(5), 645–657. https://doi.org/10.1016/S0092-8674(03)00154-5

Darzynkiewicz, Z., Gong, J. P., Juan, G., Ardelt, B., & Traganos, F. (1996). Cytometry of cyclin proteins. *Cytometry 25*,1–13. https://doi.org/10.1002/(SICI)1097-0320(19960901)25:1<1::AID-CYTO1>3.0.CO;2-N

David-Pfeuty, T., & Nouvian-Dooghe, Y. (1996). Human cyclin B1 is targeted to the nucleus in G(1) phase prior to its accumulation in the cytoplasm. *Oncogene 13*,1447–1460.

del Sal, G., Ruaro, M. E., Philipson, L., & Schneider, C. (1992). The growth arrest-specific gene, gas1, is involved in growth suppression. *Cell*, *70*(4), 595–607. https://doi.org/10.1016/0092-8674(92)90429-G

Descalzi Cancedda, F., Dozin, B., Zerega, B., Cermelli, S., & Cancedda, R. (2000). Ex-FABP: A fatty acid binding lipocalin developmentally regulated in chicken endochondral bone formation and myogenesis. *Biochimica et Biophysica Acta*, *1482*(1–2), 127–135. https://doi.org/10.1016/s0167-4838(00)00159-x

di Marco, E., Sessarego, N., Zerega, B., Cancedda, R., & Cancedda, F. D. (2003). Inhibition of cell proliferation and induction of apoptosis by ExFABP gene targeting. *Journal of Cellular Physiology*, *196*(3), 464–473. https://doi.org/10.1002/jcp.10310

Dong, Z., Wang, J. Z., Yu, F., & Venkatachalam, M. A. (2003). Apoptosis-resistance of hypoxic cells: multiple factors involved and a role for IAP-2. *The American journal of pathology*, *163*(2), 663–671. https://doi.org/10.1016/S0002-9440(10)63693-0

Dubé, A., Harrisson, J. F., Saint-Gelais, G., & Séguin, C. (2011). Hypoxia acts through multiple signaling pathways to induce metallothionein transactivation by the metal-responsive transcription factor-1 (MTF-1). *Biochemistry and cell biology = Biochimie et biologie cellulaire*, *89*(6), 562–577. https://doi.org/10.1139/o11-063

Elmore S. (2007). Apoptosis: a review of programmed cell death. *Toxicologic pathology*, *35*(4), 495–516. https://doi.org/10.1080/01926230701320337

Erb, M. (2016). *Characterizing the transcriptional regulation and role of the growth arrest specific p20K lipocalin in chicken embryo fibroblasts.* [Unpublished master's thesis]. McMaster University.

Erb, M. J., Camacho, D., Xie, W., Maslikowski, B. M., Fielding, B., Ghosh, R., Poujade, F. A., Athar, M., Assee, S., Mantella, L. E., & Bédard, P. A. (2016). Extracellular signal-regulated kinase 2 and CHOP restrict the expression of the growth arrest-specific p20K lipocalin gene to G0. *Molecular and Cellular Biology*, *36*(23), 2890–2902. https://doi.org/10.1128/MCB.00338-16

Fleming, J. V., Hay, S. M., Harries, D. N., & Rees, W. D. (1998). Effects of nutrient deprivation and differentiation on the expression of growth-arrest genes (gas and gadd) in F9 embryonal carcinoma cells. *The Biochemical Journal*, *330*(1), 573–579. https://doi.org/10.1042/bj3300573

Flower, D. R. (1996). The lipocalin protein family: Structure and function. *The Biochemical Journal*, *318*(1), 1-14. https://doi.org/10.1042/bj3180001

Fong, S. T, Camakaris, J., & Lee, B. T. O. (1995). Molecular genetics of a chromosomal locus involved in copper tolerance in *Escherichia coli* K-12. *Molecular Microbiology*, *15*(6), 1127–1137. https://doi.org/10.1111/j.1365-2958.1995.tb02286.x

Fornace, A. J., Nebert D. W., Christine Hollander,', M., Luethy, J. D., Papathanasiou, M., Fargnoli, J., & Holbrooke, N. J. (1989). Mammalian Genes Coordinately Regulated by Growth Arrest Signals and DNA-Damaging Agents. *Molecular and Cellular Biology*, *9*(10)

Gentili, C., Cermelli, S., Tacchetti, C., Cossu, G., Cancedda, R., & Cancedda, F. D. (1998). Expression of the extracellular fatty acid binding protein (Ex-FABP) during muscle fiber

formation *in vivo* and *in vitro*. *Experimental Cell Research*, *242*(2), 410–418. https://doi.org/10.1006/excr.1998.4098

Gentili, C., Tutolo, G., Zerega, B., DiMarco, E., Cancedda, R., & Descalzi Cancedda, F. (2005). Acute phase lipocalin Ex-FABP is involved in heart development and cell survival. *Journal of Cellular Physiology*, *202*(3), 683–689. https://doi.org/10.1002/jcp.20165

Giaccia, A. J., Simon, M. C., & Johnson, R. (2004). The biology of hypoxia: The role of oxygen sensing in development, normal function, and disease. *Genes and Development*, *18*(18), 2183–2194. https://doi.org/10.1101/gad.1243304

Gos, M., Miloszewska, J., Swoboda, P., Trembacz, H., Skierski, J., & Janik, P. (2005). Cellular quiescence induced by contact inhibition or serum withdrawal in C3H10T1/2 cells. *Cell Proliferation*, *38*(2), 107–116. https://doi.org/10.1111/j.1365-2184.2005.00334.x

Greijer, A. E., & van der Wall, E. (2004). The role of hypoxia inducible factor 1 (HIF-1) in hypoxia induced apoptosis. *Journal of clinical pathology*, *57*(10), 1009–1014. https://doi.org/10.1136/jcp.2003.015032

Gross, A., Yin, X. M., Wang, K., Wei, M. C., Jockel, J., Milliman, C., Erdjument-Bromage, H., Tempst, P., & Korsmeyer, S. J. (1999). Caspase cleaved BID targets mitochondria and is required for cytochrome c release, while BCL-XL prevents this release but not tumor necrosis factor-R1/Fas death. *The Journal of biological chemistry*, *274*(2), 1156–1163. https://doi.org/10.1074/jbc.274.2.1156

Guan, K. L., Jenkins, C. W., Li, Y., Nichols, M. A., Wu, X. Y., O'Keefe, C. L., Matera, A. G., & Xiong, Y. (1994). Growth suppression by p18, a p16(INK4/MTS1)- and p14(INK4B/MTS2)-related CDK6 inhibitor, correlates with wild-type pRb function. *Genes and Development 8*, 2939–2952. doi:10.1101/gad.8.24.2939

Günther, V., Lindert, U., & Schaffner, W. (2012). The taste of heavy metals: gene regulation by MTF-1. *Biochimica et biophysica acta*, *1823*(9), 1416–1425. https://doi.org/10.1016/j.bbamcr.2012.01.005

Guo, K., Searfoss, G., Krolikowski, D., Pagnoni, M., Franks, C., Clark, K., Yu, K. T., Jaye, M., & Ivashchenko, Y. (2001). Hypoxia induces the expression of the pro-apoptotic gene BNIP3. *Cell death and differentiation*, *8*(4), 367–376. https://doi.org/10.1038/sj.cdd.4400810

Guzy, R. D., Hoyos, B., Robin, E., Chen, H., Liu, L., Mansfield, K. D., Simon, M. C., Hammerling, U., & Schumacker, P. T. (2005). Mitochondrial complex III is required for hypoxia-induced ROS production and cellular oxygen sensing. *Cell metabolism*, *1*(6), 401–408. https://doi.org/10.1016/j.cmet.2005.05.001

Halliwell, B. (1991). Reactive oxygen species in living systems: Source, biochemistry, and role in human disease. *American Journal of Medicine*, *91*(3C), S14–S22. https://doi.org/10.1016/0002-9343(91)90279-7

Hamanaka, R. B., & Chandel, N. S. (2009). Mitochondrial reactive oxygen species regulate hypoxic signaling. *Current opinion in cell biology*, *21*(6), 894–899. https://doi.org/10.1016/j.ceb.2009.08.005

Hayles, J., & Nurse, P. (1986). Cell cycle regulation in yeast. *Journal of Cell Science 4*,155–170. https://doi.org/10.1242/jcs.1986.Supplement_4.10

Hirai, H., Roussel, M. F., Kato, J. Y., Ashmun, R. A., & Sherr, C. J. (1995). Novel INK4 proteins, p19 and p18, are specific inhibitors of the cyclin D-dependent kinases cdk4 and cdk6. *Molecular and Cellular Biology 15,* 2672–2681. https://doi.org/10.1128/MCB.15.5.2672

Hirst, K., Fisher, F., McAndrew, P. C., & Goding, C. R. (1994). The transcription factor, the cdk, its cyclin and their regulator: directing the transcriptional response to a nutritional signal. *European Molecular Biology Organization Journal 13,* 5410–5420. https://doi.org/10.1002/j.1460-2075.1994.tb06876.x

Hou, P., Liu, G., Zhao, Y., Shi, Z., Zheng, Q., Bu, G., Xu, H., & Zhang, Y. (2015). Role of copper and the copper-related protein CUTA in mediating APP processing and Aβ generation. *Neurobiology of Aging*, *36*(3), 1310–1315.

Hughes S. H. (2004). The RCAS vector system. *Folia biologica*, *50*(3-4), 107–119.https://www.sciencedirect.com/science/article/abs/pii/S0197458014007970?via%3Dihub

Juan, C. A., Pérez de la Lastra, J. M., Plou, F. J., & Pérez-Lebeña, E. (2021). The chemistry of reactive oxygen species (ROS) revisited: Outlining their role in biological macromolecules (DNA, lipids and proteins) and induced pathologies. *International journal of molecular sciences*, *22*(9), 4642. https://doi.org/10.3390/ijms22094642

Kalucka, J., Missiaen, R., Georgiadou, M., Schoors, S., Lange, C., De Bock, K., Dewerchin, M., & Carmeliet, P. (2015). Metabolic control of the cell cycle. *Cell cycle (Georgetown, Tex.), 14*(21), 3379–3388. https://doi.org/10.1080/15384101.2015.1090068

Kamb, A., Gruis, N. A., Weaver-Feldhaus, J., Liu, Q., Harshman, K., Tavtigian, S.V., Stockert, E., Day R. S., III, Johnson, B. E., & Skolnick, M. H. (1994). A cell cycle regulator potentially involved in genesis of many tumor types. *Science 264*, 436–440. https://doi.org/10.1126/science.8153634

Kato, J, Matsushime, H, Hiebert, SW, Ewen, ME, Sherr, CJ: Direct binding of cyclin-D to the retinoblastoma gene product (pRb) and pRb phosphorylation by the cyclin D-dependent

kinase cdk4. *Genes and Development 7*, 331–342. http://genesdev.cshlp.org/content/7/3/331

Kerr, J. F., Wyllie, A. H., & Currie, A. R. (1972). Apoptosis: a basic biological phenomenon with wide-ranging implications in tissue kinetics. *British journal of cancer*, *26*(4), 239–257. https://doi.org/10.1038/bjc.1972.33

Kill, I. R., & Hutchison, C. J. (1995). S-phase phosphorylation of lamin B2. *Federation of European Biochemical Societies Letters 377*, 26–30. https://doi.org/10.1016/0014-5793(95)01302-4

Kim, S., Mao, P. L., Gagliardi, M., & Bédard, P. A. (1999). C/EBPbeta (NF-M) is essential for activation of the p20K lipocalin gene in growth-arrested chicken embryo fibroblasts. *Molecular and Cellular Biology*, *19*(8), 5718–5731. https://doi.org/10.1128/mcb.19.8.5718

Leontieva, O. v., Natarajan, V., Demidenko, Z. N., Burdelya, L. G., Gudkov, A. v., & Blagosklonny, M. v. (2012). Hypoxia suppresses conversion from proliferative arrest to cellular senescence. *Proceedings of the National Academy of Sciences of the United States of America*, *109*(33), 13314–13318. https://doi.org/10.1073/pnas.1205690109

Liang, D., Carvalho, S., Bon, S., & Massoulié, J. (2009). Unusual transfer of CutA into the secretory pathway, evidenced by fusion proteins with acetylcholinesterase. *The FEBS journal*, *276*(16), 4473–4482. https://doi.org/10.1111/j.1742-4658.2009.07154.x

Lih, C. J., Cohen, S. N., Wang, C., & Lin-Chao, S. (1996). The platelet-derived growth factor α-receptor is encoded by a growth-arrest-specific (gas) gene. *Proceedings of the National Academy of Sciences of the United States of America*, *93*(10), 4617–4622. https://doi.org/10.1073/pnas.93.10.4617

Liu, H., Guo, H., Jian, Z., Cui, H., Fang, J., Zuo, Z., Deng, J., Li, Y., Wang, X., & Zhao, L. (2020). Copper induces oxidative stress and apoptosis in the mouse liver. *Oxidative medicine and cellular longevity, 2020*, 1359164. https://doi.org/10.1155/2020/1359164

Lodish, H., Berk, A., Zipursky, S. L., Matsudaira, P., Baltimore, D., & Darnell, J. (2000). Overview of the cell cycle and its control. In *Molecular Cell Biology*. W. H. Freeman.

Mansour, S. A., & Mossa, A. T. H. (2009). Lipid peroxidation and oxidative stress in rat erythrocytes induced by chlorpyrifos and the protective effect of zinc. *Pesticide Biochemistry and Physiology*, *93*(1), 34–39. https://doi.org/10.1016/j.pestbp.2008.09.004

Mao, P.-L., Beauchemin, M., & Bedard, P.-A. (1993). Quiescence-dependent activation of the p20K promoter in growth-arrest chickecn embryo fibroblasts. *The Journal of Biological Chemistry*, *268*(11).

McNally, F. J. (1996). Modulation of microtubule dynamics during the cell cycle. *Current Opinion in Cell Biology 8*,23–29. https://doi.org/10.1016/S0955-0674(96)80044-5

Melkonyan, H. S., Chang, W. C., Shapiro, J. P., Mahadevappa, M., Fitzpatrick, P. A., Kiefer, M. C., Tomei, L. D., & Umansky, S. R. (1997). SARPs: A family of secreted apoptosis-related proteins. *Proceedings of the National Academy of Sciences of the United States of America*, *94*(25), 13636–13641. https://doi.org/10.1073/pnas.94.25.13636

Mishra, O. P., & Delivoria-Papadopoulos, M. (1989). Lipid peroxidation in developing fetal guinea pig brain during normoxia and hypoxia. *Developmental Brain Research*, *45*(1), 129–135. https://doi.org/10.1016/0165-3806(89)90014-X

Moftakhari, R., Donders, J., Erb, M. J., Peragine, S., Sriranjan, S., Moriniti, J., & Bedard, P.-A. (2022). *Lipocalins alleviate oxidative stress to promote cell survival and growth arrest-*

specific gene expression in quiescent chicken embryo fibroblasts. Unpublished manuscript.

Murphy B. J. (2004). Regulation of malignant progression by the hypoxia-sensitive transcription factors HIF-1alpha and MTF-1. *Comparative biochemistry and physiology. Part B, Biochemistry & molecular biology*, *139*(3), 495–507. https://doi.org/10.1016/j.cbpc.2004.04.009

Murphy, B. J., Andrews, G. K., Bittel, D., Discher, D. J., McCue, J., Green, C. J., Yanovsky, M., Giaccia, A., Sutherland, R. M., Laderoute, K. R., & Webster, K. A. (1999). Activation of metallothionein gene expression by hypoxia involves metal response elements and metal transcription factor-1. *Cancer research*, *59*(6), 1315–1322.

Murphy, B. J., Kimura, T., Sato, B. G., Shi, Y., & Andrews, G. K. (2008). Metallothionein induction by hypoxia involves cooperative interactions between metal-responsive transcription factor-1 and hypoxia-inducible transcription factor-1alpha. *Molecular cancer research : MCR*, *6*(3), 483–490. https://doi.org/10.1158/1541-7786.MCR-07-0341

Murphy, B. J., Sato, B. G., Dalton, T. P., & Laderoute, K. R. (2005). The metal-responsive transcription factor-1 contributes to HIF-1 activation during hypoxic stress. *Biochemical and biophysical research communications*, *337*(3), 860–867. https://doi.org/10.1016/j.bbrc.2005.09.124

Navaratnam, D. S., Fernando, F. S., Priddle, J. D., Giles, K., Clegg, S. M., Pappin, D. J., Craig, I., & Smith, A. D. (2000). Hydrophobic protein that copurifies with human brain acetylcholinesterase: amino acid sequence, genomic organization, and chromosomal localization. *Journal of neurochemistry*, *74*(5), 2146–2153. https://doi.org/10.1046/j.1471-4159.2000.0742146.

Norbury, C. J., & Hickson, I. D. (2001). Cellular responses to DNA damage. *Annual review of pharmacology and toxicology*, *41*, 367–401. https://doi.org/10.1146/annurev.pharmtox.41.1.367

Opazo, C., Barría, M., Ruiz, F, Inestrosa, N. (2003). Copper reduction by copper binding proteins and its relation to neurodegenerative diseases. *Biometals 16*, 91–98. https://doi.org/10.1023/A:1020795422185

Pack, L. R., Daigh, L. H., & Meyer, T. (2019). Putting the brakes on the cell cycle: Mechanisms of cellular growth arrest. *Current Opinion in Cell Biology 60*, 106–113. https://doi.org/10.1016/j.ceb.2019.05.005

Pines J. (1991). Cyclins: wheels within wheels. *Cell growth & differentiation: the molecular biology journal of the American Association for Cancer Research*, *2*(6), 305–310. https://pubmed.ncbi.nlm.nih.gov/1648379/

Pines, J. (1995). Cyclins and cyclin-dependent kinases: theme and variations. *Advances in Cancer Research 66*,181–212. https://doi.org/10.1016/S0065-230X(08)60254-7

Rensing, C., & Grass, G. (2003). *Escherichia coli* mechanisms of copper homeostasis in a changing environment. *FEMS Microbiology Reviews*, *27*(2–3), 197–213. https://doi.org/10.1016/S0168-6445(03)00049-4

Reynolds, T. Y., Rockwell, S., & Glazer, P. M. (1996). Genetic instability induced by the tumor microenvironment. *Cancer research*, *56*(24), 5754–5757.

Ribatti, D. (2017). A revisited concept: Contact inhibition of growth. From cell biology to malignancy. *Experimental Cell Research*, *359*(1), 17–19. https://doi.org/10.1016/j.yexcr.2017.06.012

Schafer K. A. (1998). The cell cycle: a review. *Veterinary pathology*, *35*(6), 461–478. https://doi.org/10.1177/030098589803500601

Schneider, C., King, R. M., & Philipson, L. (1988). Genes specifically expressed at growth arrest of mammalian cells. *Cell*, *54*(6), 787–793. https://doi.org/10.1016/S0092-8674(88)91065-3

Selim, K. A., Tremiño, L., Marco-Marín, C., Alva, V., Espinosa, J., Contreras, A., Hartmann, M. D., Forchhammer, K., & Rubio, V. (2021). Functional and structural characterization of PII-like protein CutA does not support involvement in heavy metal tolerance and hints at a small-molecule carrying/signaling role. *The FEBS journal*, *288*(4), 1142–1162. https://doi.org/10.1111/febs.15464

Shambaugh, G. E., 3rd, Lee, R. J., Watanabe, G., Erfurth, F., Karnezis, A. N., Koch, A. E., Haines, G. K., 3rd, Halloran, M., Brody, B. A., & Pestell, R. G. (1996). Reduced cyclin D1 expression in the cerebella of nutritionally deprived rats correlates with developmental delay and decreased cellular DNA synthesis. *Journal of neuropathology and experimental neurology*, *55*(9), 1009–1020. https://doi.org/10.1097/00005072-199609000-00008

Shimoda, R., Achanzar, W. E., Qu, W., Nagamine, T., Takagi, H., Mori, M., & Waalkes, M. P. (2003). Metallothionein is a potential negative regulator of apoptosis. *Toxicological sciences : an official journal of the Society of Toxicology*, *73*(2), 294–300. https://doi.org/10.1093/toxsci/kfg095

Środa-Pomianek, K., Michalak, K., Świątek, P., Poła, A., Palko-Łabuz, A., & Wesołowska, O. (2018). Increased lipid peroxidation, apoptosis and selective cytotoxicity in colon cancer cell line LoVo and its doxorubicin-resistant subline LoVo/Dx in the presence of newly

synthesized phenothiazine derivatives. *Biomedicine & pharmacotherapy = Biomedecine & pharmacotherapie, 106,* 624–636. https://doi.org/10.1016/j.biopha.2018.06.170

Su, L. J., Zhang, J. H., Gomez, H., Murugan, R., Hong, X., Xu, D., Jiang, F., & Peng, Z. Y. (2019). Reactive oxygen species-induced lipid peroxidation in apoptosis, autophagy, and ferroptosis. *Oxidative medicine and cellular longevity*, *2019*, 5080843. https://doi.org/10.1155/2019/5080843

Tanaka, Y., Tsumoto, K., Nakanishi, T., Yasutake, Y., Sakai, N., Yao, M., Tanaka, I. & Kumagai, I. (2004). Structural implications for heavy metal-induced reversible assembly and aggregation of a protein: The case of *Pyrococcus horikoshii* CutA 1. *FEBS Letters*, *556*(1-3), 167–174. https://doi.org/10.1016/S0014-5793(03)01402-9

Terzi, M. Y., Izmirli, M., & Gogebakan, B. (2016). The cell fate: Senescence or quiescence. *Molecular Biology Reports*, 43(11), 1213–1220.https://doi.org/10.1007/s11033-016-4065-0

van den Heuvel, S., & Harlow, E. (1993). Distinct roles for cyclin-dependent kinases in cell cycle control. *Science (New York, N.Y.)*, *262*(5142), 2050–2054. https://doi.org/10.1126/science.8266103

van Deursen, J. M. (2014). The role of senescent cells in ageing. *Nature*,*509*(7501), 439–446. https://doi.org/10.1038/nature13193

Vaupel, P. (2004). The role of hypoxia-induced factors in tumor progression. *The Oncologist*, *9*(suppl 5), 10–17. https://doi.org/10.1634/theoncologist.9-90005-10

Vermeulen, K., Berneman, Z. N., & van Bockstaele, D. R. (2003). Cell cycle and apoptosis. *Cell Proliferation*,*36*(3),165–175. https://doi.org/10.1046/j.1365-2184.2003.00267.x

Yang X. J. (2002). Retrovirus-mediated gene expression during chick visual system development. *Methods (San Diego, Calif.)*, *28*(4), 396–401. https://doi.org/10.1016/s1046-2023(02)00258-x

Yang, J., Yang, H., Yan, L., Yang, L., & Yu, L. (2009). Characterization of the human CUTA isoform2 present in the stably transfected HeLa cells. *Molecular biology reports*, *36*(1), 63–69. https://doi.org/10.1007/s11033-007-9152-9

Yin, H., Xu, L., & Porter, N. A. (2011). Free radical lipid peroxidation: mechanisms and analysis. *Chemical reviews*, *111*(10), 5944–5972. https://doi.org/10.1021/cr200084z

Zegers, M. M. P., Forget, M.A., Chernoff, J., Mostov, K. E., ter Beest, M. B. A., & Hansen, S. H. (2003). Pak1 and PIX regulate contact inhibition during epithelial wound healing. *The EMBO Journal*, *22*(16), 4155–4165. https://doi.org/10.1093/emboj/cdg398

Zhao, Y., Wang, Y., Hu, J., Zhang, X., & Zhang, Y. W. (2012). CutA divalent cation tolerance homolog (*Escherichia coli*) (CUTA) regulates β-cleavage of β-amyloid precursor protein (APP) through interacting with β-site APP cleaving protein 1 (BACE1). *Journal of Biological Chemistry*, *287*(14), 11141–11150. https://doi.org/10.1074/jbc.M111.330209